Bioorganic Chemistry

Biotinylated selenocyanates: potent and selective cytostatic agents

--Manuscript Draft--

Manuscript Number:	
Article Type:	Full Length Article
Keywords:	biotin; organochalcogen; selenocyanate; antiproliferative; apoptosis; cytostatic agent
Corresponding Author:	Óscar López Universidad de Sevilla Seville, SPAIN
First Author:	Jesús M. Roldán-Peña
Order of Authors:	Jesús M. Roldán-Peña
	Adrián Puerta
	Jelena Dinić
	Sofija Jovanović Stojanov
	Aday González-Bakker
	Francisco J. Hicke
	Atreyee Mishra
	Akkharadet Piyasaengthong
	Inés Maya
	James W. Walton
	Milica Pešić
	José M. Padrón
	José G. Fernández-Bolaños
	Óscar López
Abstract:	Most of the currently available cytotoxic agents for tackling cancer are devoid of selectivity, thus causing severe side-effects. This situation stimulated us to develop new antiproliferative agents with enhanced affinity towards tumour cells. For that purpose, we envisioned the possibility of conjugating, through a peptide linkage, an organochalcogen motif (thiosemicarbazones, disulfides, selenoureas, thio- and selenocyanates), with biotin (vitamin B7), a cellular growth promoter, whose receptor is overexpressed in numerous cancer cells. Accordingly, the biotin residue can act as a selective vector towards malignant cells. We prepared a biotinylated selenocyanate that behaved as a very strong antiproliferative agent, achieving GI50 values in the low nM range for most of the tested cancer cells; moreover, it was featured with an outstanding selectivity, with GI50 > 100 μM against human fibroblasts. Mechanistic studies on the mode of inhibition of the biotinylated selenocyanate revealed (Annexin-V assay) a remarkable increase in the number of apoptotic cells compared to the control experiment; moreover, depolarization of the mitochondrial membrane was detected by flow cytometry analysis, and with fluorescent microscopy, what supports the apoptotic cell death. Prior to the apoptotic events, cytostatic effects were observed against SW1573 cells using label-free cell-living imaging; therefore, tumour cell division was prevented. Multidrug resistant cell lines exhibited a reduced sensitivity towards the biotinylated selenocyanate, probably due to its P-gp-mediated efflux. Remarkably, antiproliferative levels could be restored by co-administration with tariquidar, a P-gp inhibitor; this approach can, therefore, overcome multidrug resistance mediated by the P-gp efflux system.
Suggested Reviewers:	Carmen Sanmartín, Dr.

	Full Professor, University of Navarra sanmartin@unav.es Expert in organoselenium chemistry with biological activities, including antiproliferative properties
	Igor Opsenica, Dr. Full Professor, University of Belgrade Faculty of Chemistry igorop@chem.bg.ac.rs Expert in Medicinal Chemistry
	Cristiane Luchese, Dr. Federal University of Pelotas cristiane_luchese@yahoo.com.br Expert in organoselenium chemistry with biological activities
	Fabrizio Carta, Dr. University of Florence fabrizio.carta@unifi.it Expert in Medicinal Chemistry for the treatment of multifactorial pathologies.
	Michael S. Christodoulou, Dr. University of Milan michalis.christ@gmail.com Expert in antitumour agents
Opposed Reviewers:	

Department of Organic Chemistry
Faculty of Chemistry, University of Seville
c/ Profesor García González 1.
41012. Sevilla (Spain)
Óscar López
Associate Professor
Tel. +34 954553877
e-mail: osc-lopez@us.es

Dear Editor,

We would like you to consider our manuscript entitled "Biotinylated selenocyanates: potent and selective cytostatic agents", authored by Jesús M. Roldán-Peña, Adrián Puerta, Jelena Dinić, Sofija Jovanović Stojanov, Aday González-Bakker, Francisco J. Hicke, Atreyee Mishra, Akkharadet Piyasaengthong, Inés Maya, James W. Walton, Milica Pešić, José M. Padrón, José G. Fernández-Bolaños, Óscar López for the publication in Bioorganic Chemistry journal.

Herein we have accomplished the conjugation of D-biotin (vitamin B_7) with a series of organochalcogen derivatives (thiosemicarbazones, disulfides, selenoureas, thio- and selenocyanates) with the aim of developing selective antitumour agents, based on the fact that biotin receptors are overexpressed in numerous malignant cells.

This approach turned out to be particularly effective in the case of selenocyanates, providing a very strong and selective antiproliferative agent, with activities reaching the nM range in six out of the seven human tumour cell lines tested, and outstanding selectivities.

Apoptosis and depolarization of the mitochondria membrane were found to be involved in the mode of action of biotinylated selenocyanate. Prior to the apoptotic events, cytostatic effects were observed against SW1573 cells using label-free cell-living imaging; therefore, tumour cell division was prevented. Moreover, co-administration with tariquidar turned out to be a valid approach to avoid P-gp-mediated chemoresistance,

For all these reasons, we think that the disclosure of these results can be of interest for the scientific community.

Thank you very much for your consideration.

Yours sincerely,

Óscar López

Biotinylated selenocyanates: potent and selective cytostatic agents

Jesús M. Roldán-Peña,[a] Adrián Puerta[b], Jelena Dinić,[c] Sofija Jovanović Stojanov,[c] Aday González-Bakker,[b] Francisco J. Hicke,[a] Atreyee Mishra,[d] Akkharadet Piyasaengthong,[d,e] Inés Maya,[a] James W. Walton,[d] Milica Pešić,[c,*] José M. Padrón,[b,*] José G. Fernández-Bolaños,[a,*] Óscar López[a,*]

[a]*Organic Chemistry Department, Faculty of Chemistry, University of Seville, PO box 1203, E-41071 Seville, Spain. e-mail: bolanos@us.es, osc-lopez@us.es*

[b]*BioLab, Instituto Universitario de Bio-Orgánica "Antonio González" (IUBO-AG), Universidad de La Laguna, Astrofísico Francisco Sánchez 2, E-38206 La Laguna, Spain, e-mail: jmpadron@ull.es*

[c]*Institute for Biological Research "Siniša Stanković", National Institute of the Republic of Serbia, University of Belgrade, Despota Stefana 142, 11060 Belgrade, Serbia, e-mail: camala@ibiss.bg.ac.rs*

[d]*Department of Chemistry, Durham University, Lower Mountjoy, South Road, Durham DH1 3LE, UK*

[e]*Bioscience Program, Faculty of Science, Kasetsart University, Bangkok 10900, Chatuchak, Thailand*

Highlights

- Biotinylation of the pharmacophore selenocyanate led to a very strong antiproliferative agent
- Nanomolar activities were obtained in most of the tested cell lines for the lead compound
- Outstanding selectivities were achieved (S.I. up to > 7700)
- Depolarization of tumour mitochondrial membrane, leading to apoptosis was observed
- MDR cells were efficiently targeted by co-administration with tariquidar
- Cytostatic action was observed for the lead compound against SW1573 cells using continuous cell-living imaging

Graphical Abstract

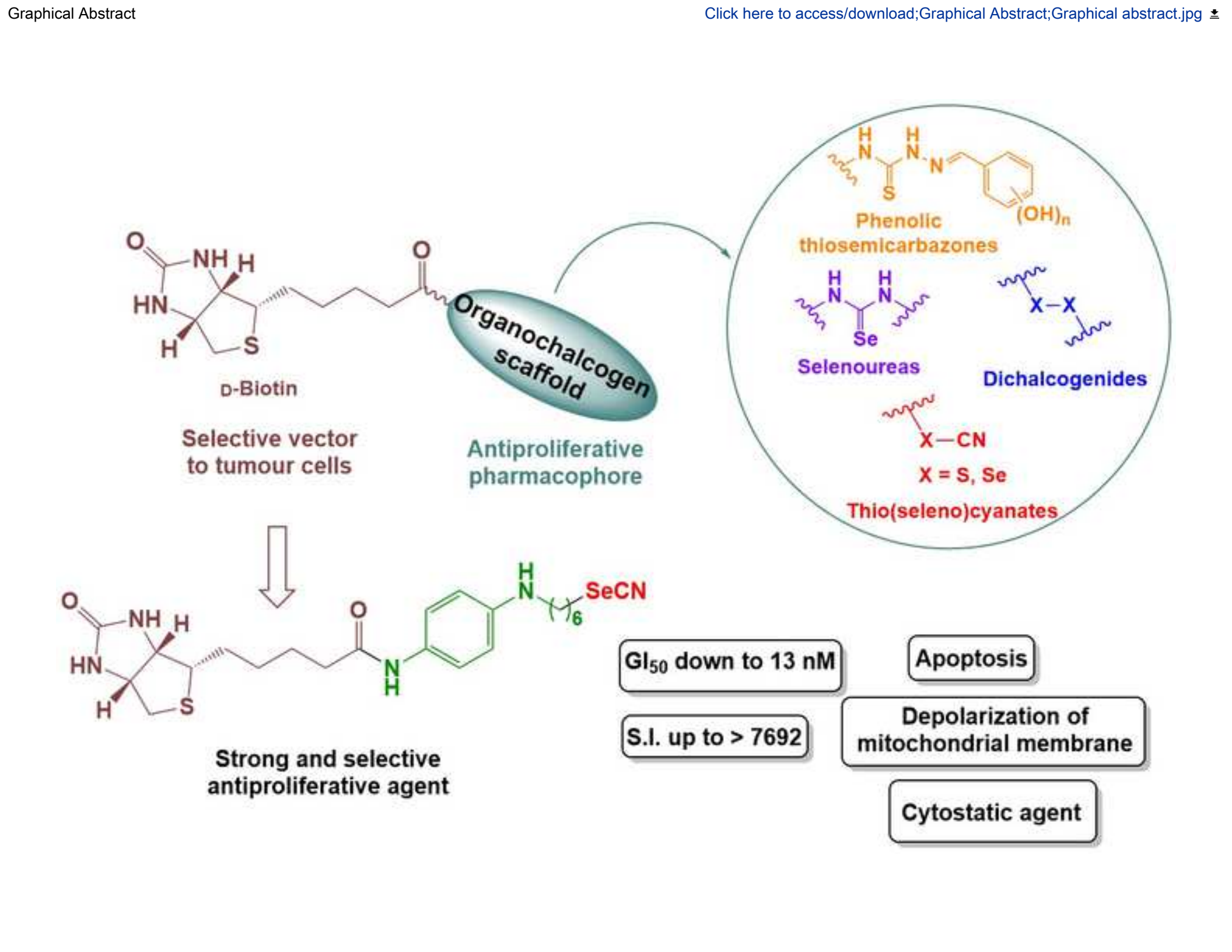

Biotinylated selenocyanates: potent and selective cytostatic agents

Jesús M. Roldán-Peña,[a] Adrián Puerta,[b] Jelena Dinić,[c] Sofija Jovanović Stojanov,[c] Aday González-Bakker,[b] Francisco J. Hicke,[a] Atreyee Mishra,[d] Akkharadet Piyasaengthong,[d,e] Inés Maya,[a] James W. Walton,[d] Milica Pešić,[c,*] José M. Padrón,[b,*] José G. Fernández-Bolaños,[a,*] Óscar López[a,*]

[a]*Organic Chemistry Department, Faculty of Chemistry, University of Seville, PO box 1203, E-41071 Seville, Spain. e-mail: bolanos@us.es, osc-lopez@us.es*

[b]*BioLab, Instituto Universitario de Bio-Orgánica "Antonio González" (IUBO-AG), Universidad de La Laguna, Astrofísico Francisco Sánchez 2, E-38206 La Laguna, Spain, e-mail: jmpadron@ull.es*

[c]*Institute for Biological Research "Siniša Stanković", National Institute of the Republic of Serbia, University of Belgrade, Despota Stefana 142, 11060 Belgrade, Serbia, e-mail: camala@ibiss.bg.ac.rs*

[d]*Department of Chemistry, Durham University, Lower Mountjoy, South Road, Durham DH1 3LE, UK*

[e]*Bioscience Program, Faculty of Science, Kasetsart University, Bangkok 10900, Chatuchak, Thailand*

Graphical abstract

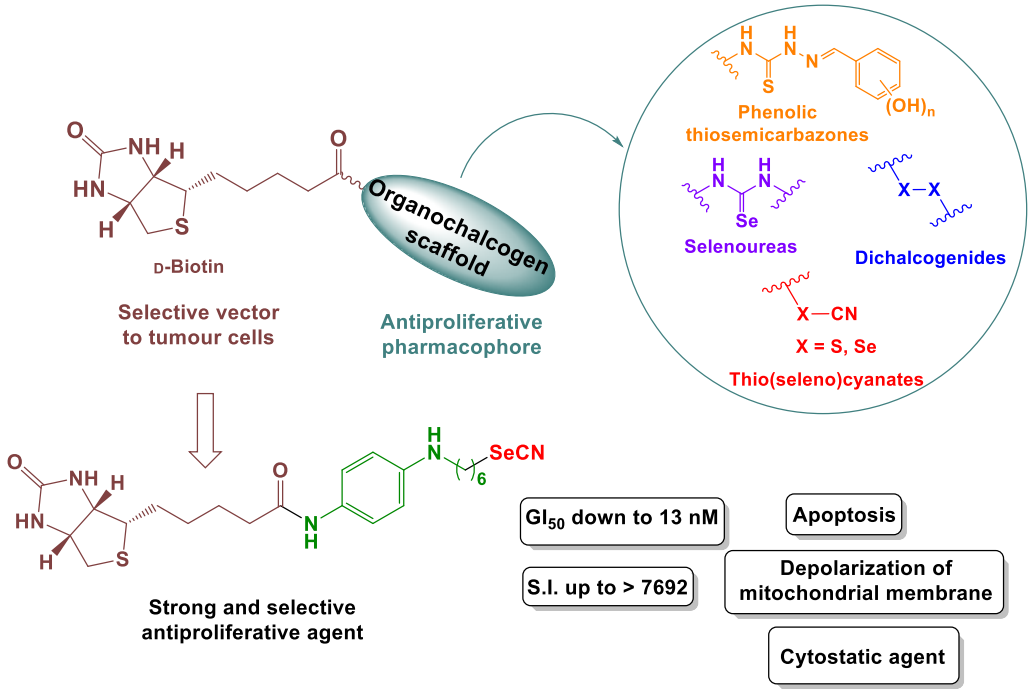

Highlights

- Biotinylation of the pharmacophore selenocyanate led to a very strong antiproliferative agent
- Nanomolar activities were obtained in most of the tested cell lines for the lead compound
- Outstanding selectivities were achieved (S.I. up to > 7700)
- Depolarization of tumour mitochondrial membrane, leading to apoptosis was observed
- MDR cells were efficiently targeted by co-administration with tariquidar
- Cytostatic action was observed for the lead compound against SW1573 cells using continuous cell-living imaging

Abstract

Most of the currently available cytotoxic agents for tackling cancer are devoid of selectivity, thus causing severe side-effects. This situation stimulated us to develop new antiproliferative agents with enhanced affinity towards tumour cells. For that purpose, we envisioned the possibility of conjugating, through a peptide linkage, an organochalcogen motif (thiosemicarbazones, disulfides, selenoureas, thio- and selenocyanates), with biotin (vitamin B_7), a cellular growth promoter, whose receptor is overexpressed in numerous cancer cells. Accordingly, the biotin residue can act as a selective vector towards malignant cells. We prepared a biotinylated selenocyanate that behaved as a very strong antiproliferative agent, achieving GI_{50} values in the low nM range for most of the tested cancer cells; moreover, it was featured with an outstanding selectivity, with GI_{50} > 100 μM against human fibroblasts.

Mechanistic studies on the mode of inhibition of the biotinylated selenocyanate revealed (Annexin-V assay) a remarkable increase in the number of apoptotic cells compared to the control experiment; moreover, depolarization of the mitochondrial membrane was detected by flow cytometry analysis, and with fluorescent microscopy, what supports the apoptotic cell death. Prior to the apoptotic events, cytostatic effects were observed against SW1573 cells using label-free cell-living imaging; therefore, tumour cell division was prevented.

Multidrug resistant cell lines exhibited a reduced sensitivity towards the biotinylated selenocyanate, probably due to its P-gp-mediated efflux. Remarkably, antiproliferative levels could be restored by co-administration with tariquidar, a P-gp inhibitor; this approach can, therefore, overcome multidrug resistance mediated by the P-gp efflux system.

Keywords: biotin, organochalcogen, selenocyanate, antiproliferative, apoptosis; cytostatic agent

1. Introduction

Cancer, a conglomerate of over 100 different diseases [1], depending on the tissue or organ affected, is nowadays a leading cause of morbidity and mortality worldwide [2]. In fact, cancer became in 2019 the first or second cause of death in more than 100 countries for people below 70 years old [3]. This rise is partially due to the decrease in mortality provoked by cardiovascular diseases. In 2020, 19.3 million new cancer cases and roughly 10 million deaths were estimated [3], and cancer screening was strongly hampered by COVID19 pandemic [4]. In low-income countries, roughly 30% of cancer incidence has its origin in cancer-causing infections, like hepatitis and human papillomavirus (HPV) [5].

The enormous complexity of this multifactorial disease, with etiologies not even fully understood [6], together with the severe side-effects caused by most of the chemotherapeutic agents due to lack of selectivity [7], the development of multidrug resistance (MDR) [8] or the high economic burden underwent by the patient and the society (in this context, the term *financial toxicity* was coined) [9] are some of the key aspects to be faced by the new anticancer therapies. Such therapies seek the more efficient elimination of tumour cells, the increase of rate survival and the improvement of the patient's life quality. Several recent outstanding advances in cancer treatment can be highlighted, in the attempt of boosting the immune system against tumour cells [10]; among such strategies, monoclonal antibodies for the development of cancer vaccines [11], personalized anticancer therapies by reprogramming T-cells (chimeric antigen receptor T, CAR-T, cells therapy) [12], or immune checkpoint blockades [13] are remarkable. However, primary tumour treatment still requires the use of cytotoxic agents in most of the cases; in this context, the US FDA approved 332 anticancer drugs in the period 2009–2020 [14].

Herein, we pursued the preparation of potential drug candidates to increase the arsenal of cytotoxic agents available so far. For that purpose, we envisioned the possibility of using organochalcogen derivatives; sulfur- and selenium-containing compounds exhibit a plethora of beneficial biological activities, which are frequently enhanced in the selenium isosters. Selenium is present in the active site of 25 selenoproteins, most of them belonging to the antioxidant protective machinery, and is currently considered to be an essential micronutrient, whose deficit leads to several diseases and disorders [15]. Among the numerous biological properties found in

organoselenium derivatives [16, 17], the following ones can be highlighted: strong redox properties [18], antiviral (including anti-SARS-COV-2 effects) [19], antidepressant-like properties [20], anti-inflammatory [21], antinociceptive [22], antiprotozoal [23, 24], therapeutic enzymes inhibitors like those against monoamino oxidase (MAO) and/or carbonic anhydrases [25, 26], *O*-GlcNAcase (OGA) and/or cholinesterases [27, 28], histone deacetylases (HDACs) [29, 30], or glycosidases [31], reduction of Aβ aggregation [32], or anticancer activities [33–40], among others.

In order to enhance the selectivity towards tumour cells, we envisioned the possibility of conjugating the organoselenium motif to a residue of biotin (vitamin B_7), a cell growth promoter; biotin receptor is overexpressed in numerous cancer cell lines [41], and is therefore, considered as an attractive therapeutic target for the selective vectorization of drugs towards cancer cells. Biotinylation of cytotoxic agents, like taxoids [42], doxorubicin [43], or gemcitabine [44], among others, has successfully been reported.

2. Results and discussion

2.1. Chemistry

In the search for more selective antiproliferative agents, we decided to carry out the conjugation of biotin to organochalcogen scaffolds, pharmacophores widely employed in our group [23, 27–29, 31, 39, 40]. Thus, connection with phenolic thio(seleno)semicarbazones, selenoureas, thio(selenocyanates), and disulfides/diselenides was envisioned (Figure 1).

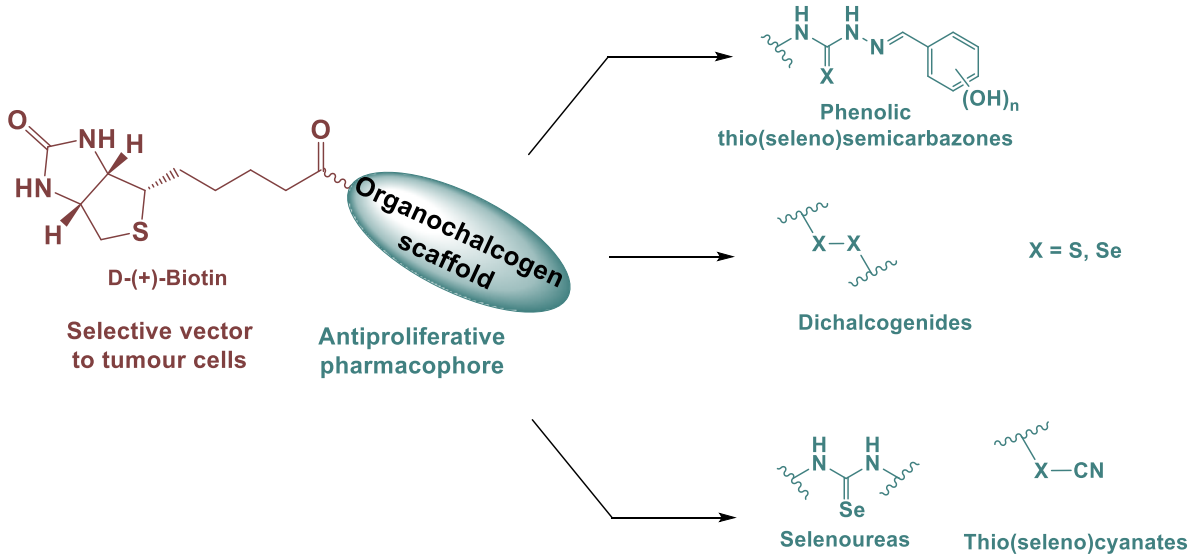

Figure 1. General structure of the biotinylated organochalcogen derivatives attempted herein

Biotin and the active pharmacophores were connected through an amide-containing linker; although the use of thionyl chloride has been reported [45] to generate the corresponding acyl chloride and the subsequent transformation into amides, the intrinsic high instability of this biotin-derived intermediate encouraged us to use a more versatile synthetic pathway. We then shifted to the activation of the carbonyl group with isobutyl chloroformate, previously used by Zheng *et al.* for linking biotin and γ-aminobutiric acid [46], followed by coupling of the transient mixed anhydride with *p*-phenylenediamine (Scheme 1).

In this context, Scheme 1 depicts conjugation of biotin with phenolic thiosemicarbazones (derivatives **9**–**11**) in five steps: activation of the carbonyl group, coupling with the aromatic diamine **3**, transformation of the free amino group of **4** into isothiocyanate **5** (using thiophosgene as the thionating agent in a triphasic medium), treatment with hydrazine and condensation of the transient thiosemicarbazide with commercially-available phenolic aldehydes **6**–**8** with different numbers of hydroxyl groups. Such phenolic scaffold is endowed with strong redox properties, and has previously used in our group to develop antiproliferative agents [40].

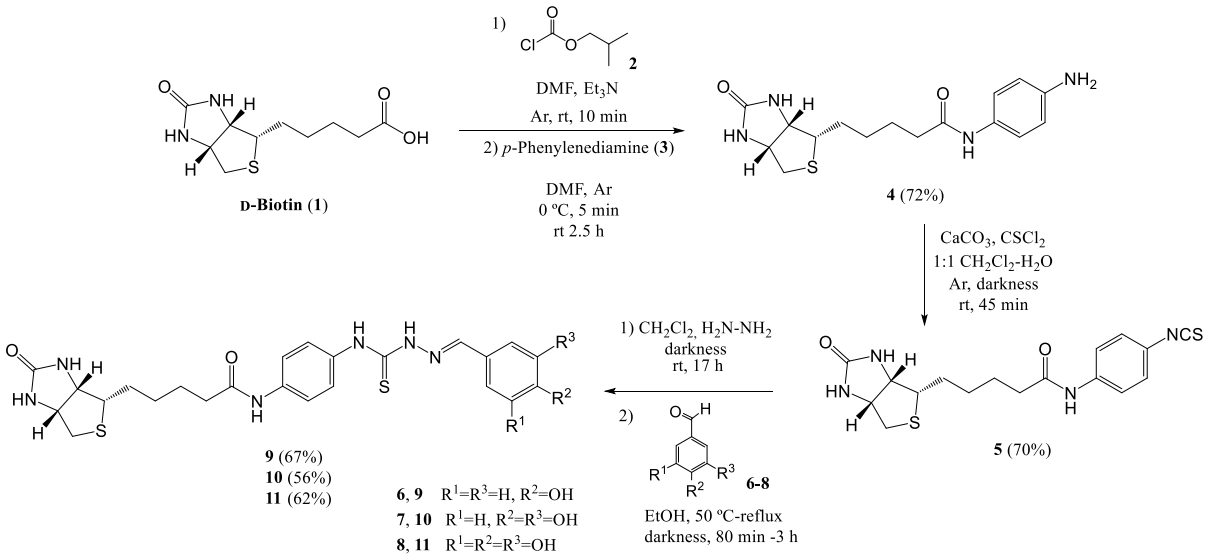

Scheme 1. Preparation of biotinylated thiosemicarbazones **9**–**11**

With the aim of analysing the influence of the biotin residue on the antiproliferative activity, thiosemicarbazone **15** was also accessed (Scheme 2); in this case, the biotinyl residue was replaced by a Boc fragment. For that purpose, monoprotection of *p*-phenylenediamine with $(Boc)_2O$ was achieved using the methodology reported by Togashi *et al.* [47]. In a similar way as depicted in Scheme 1, subsequent treatment with thiophosgene, hydrazine and 3,4-dihydroxybenzaldehyde (protocatechuic aldehyde) afforded **15** (16% overall yield, four steps).

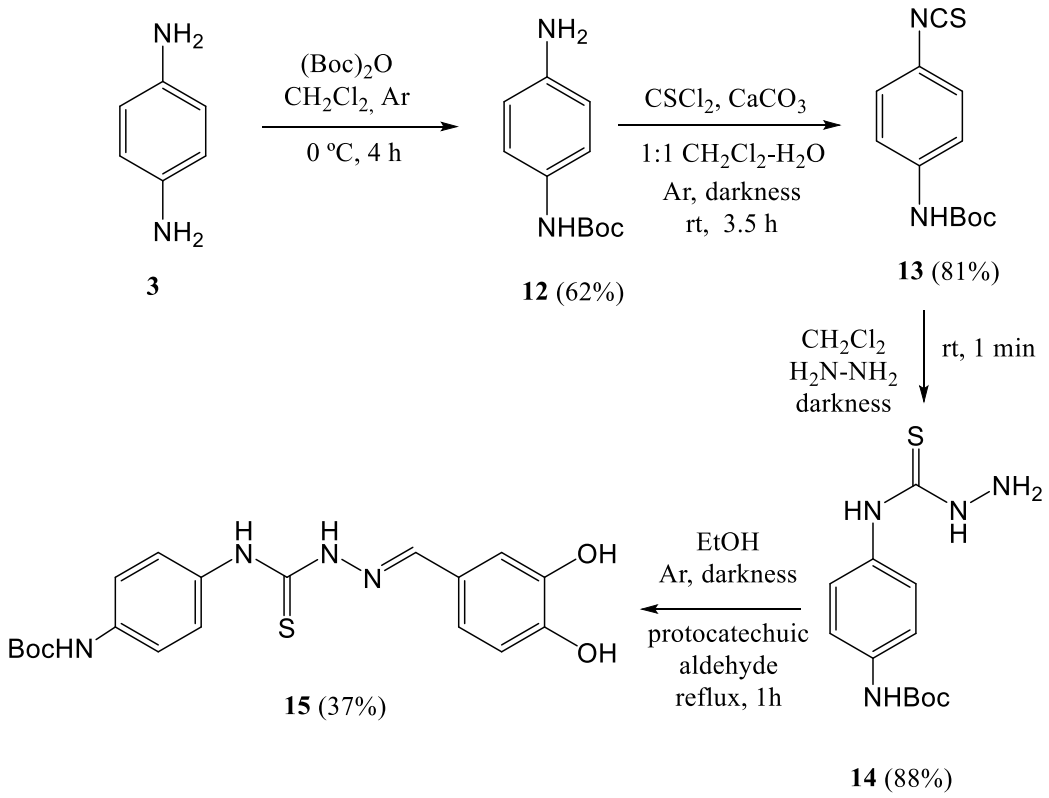

Scheme 2. Preparation of *N*-Boc-protected thiosemicarbazone **15**

The influence of the free or protected phenolic hydroxyl groups on the bioactivity was also evaluated; for that purpose, 3,4-dihydroxybenzaldehyde was acetylated prior to conjugation with biotin (compound **17**, Scheme 3). This can provide information about the potential effect of increasing the lipophilicity of the molecule.

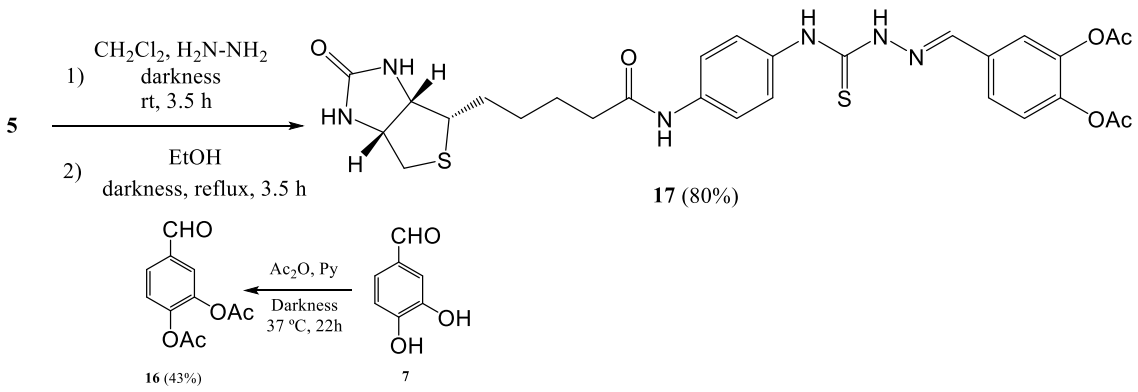

Scheme 3. Preparation of *O*-protected biotinylated thiosemicarbazone **17**

Other functionalities connected to the biotin residue were the thiocyanate and disulfide scaffolds (Scheme 4). Initially, the use of Boc-protecting group was attempted. Thus, *N*-alkylation of **12** with 1,6-dibromohexane, and subsequent nucleophilic reaction with KSCN furnished thiocyanate **19** in good yield; unfortunately, attempts to carry out the acidic deprotection of the *N*-Boc moiety were unsuccessful, as extensive decomposition was observed.

We then shifted to the use of enamine as the *N*-protecting group by coupling *p*-phenylenediamine **3** with diethyl ethoxymethylenemalonate [48] (Scheme 4). Following this approach, and starting from **20**, targeted thiocyanate **23**, with the free *p*-amino group could be successfully accessed in a three-step procedure: *N*-alkylation, nucleophilic displacement with KSCN and efficient *N*-deprotection with ethylenediamine. The presence of the thiocyanato motif was evidenced in compounds **19**, **22** and **23** in the ^{13}C-NMR spectra (resonances at 112.4–112.5 ppm).

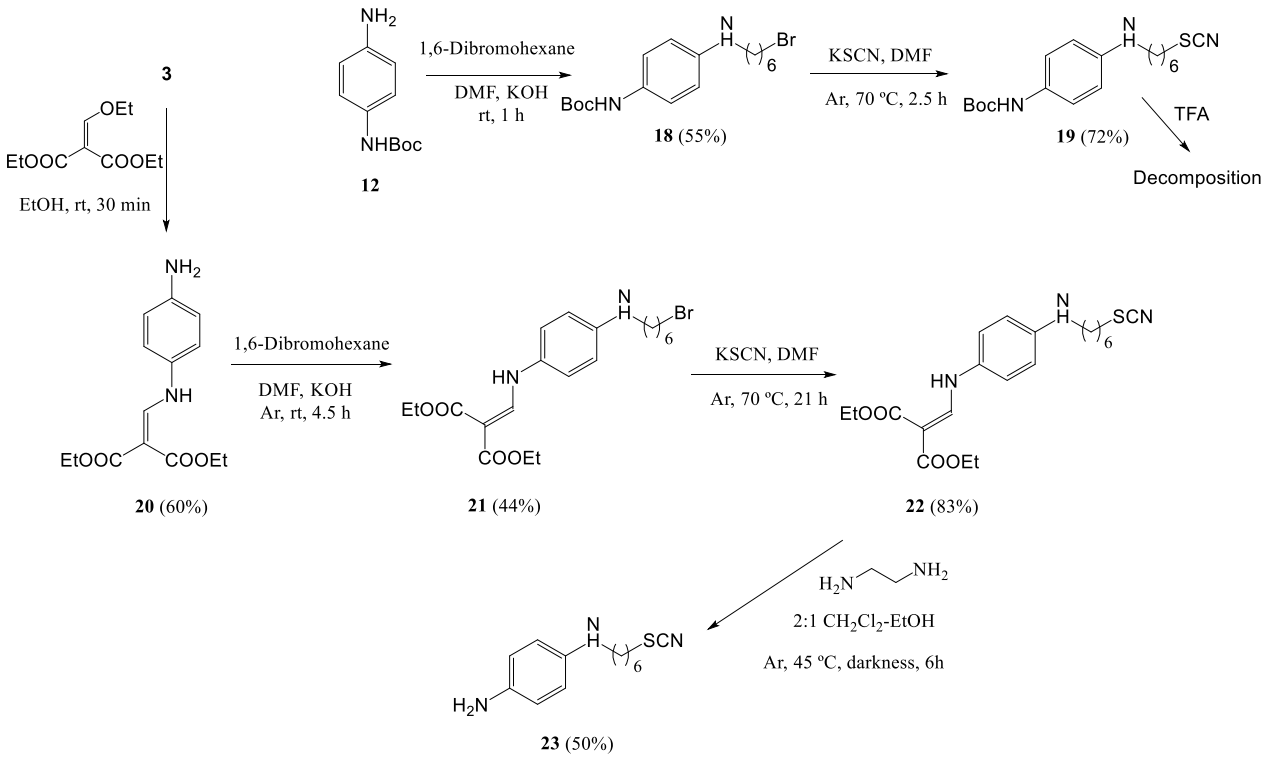

Scheme 4. Preparation of of *N*-protected and *N*-unprotected thiocyanates **19**, **22**, **23**

Next, thiocyanate **23** was conjugated to biotin using again isobutyl chloroformate as the amide coupling reagent (Scheme 5), affording biotinylated derivative **24** with a moderate yield (53%); successful transformation into dimeric disulfide **25** was achieved upon reaction with $NaBH_4$. ^{13}C-NMR spectrum of such compound revealed the absence of the resonance associated to the SCN functionality.

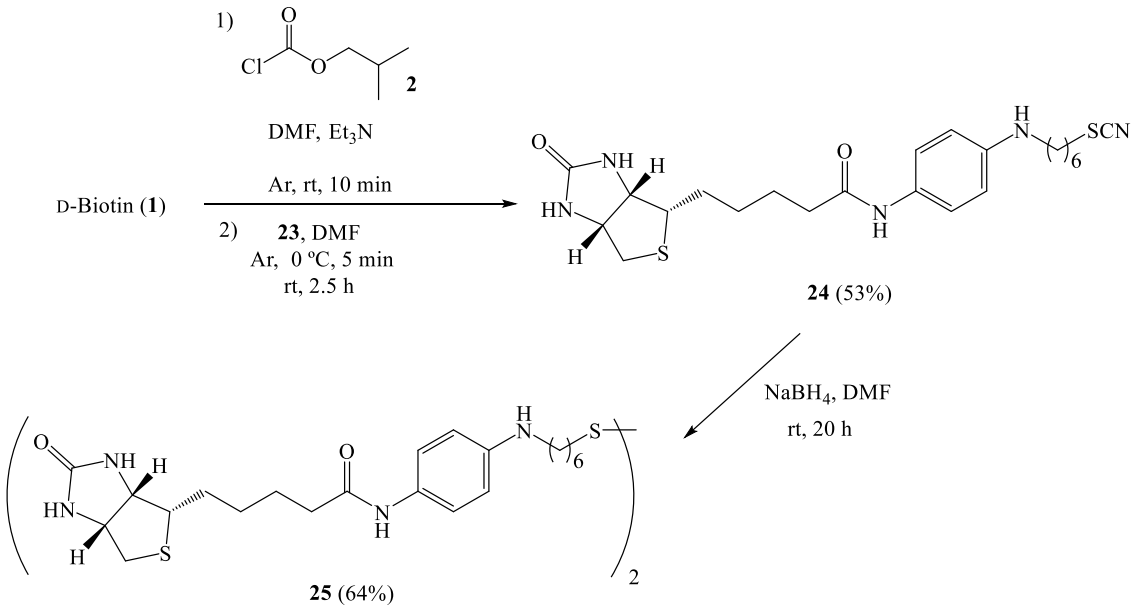

Scheme 5. Preparation of biotinylated thiocyanate **24** and disulfide **25**

The corresponding seleno-isosters were also attempted with the aim of analysing the influence of the sulfur and selenium atoms on the biological properties. Attempts to prepare biotin-derived selenosemicarbazones revealed to be unsuccessful. Thus, although the free amino derivative of **4** was transformed into the corresponding formamide with refluxing ethyl formate in almost quantitative yield (98%), treatment with triphosgene for accomplishing the dehydration of the formamide [49], followed by *in situ* coupling with elemental selenium black led, not to the expected isoselenocyanate, but to a complex and non-resolved mixture (Scheme 6). NMR analysis of some of the isolated products by column chromatography revealed the absence of the typical signals of the biotin residue, suggesting that such moiety was probably degraded under the reaction conditions.

Alternatively, direct coupling of **4** with *p*-iodophenyl isoselenocyanate furnished the expected selenourea **27** in moderate yield (57%). Resonance at 179 ppm in the ^{13}C-NMR spectrum, assigned to the selenoxo group, confirmed the structure (Scheme 6).

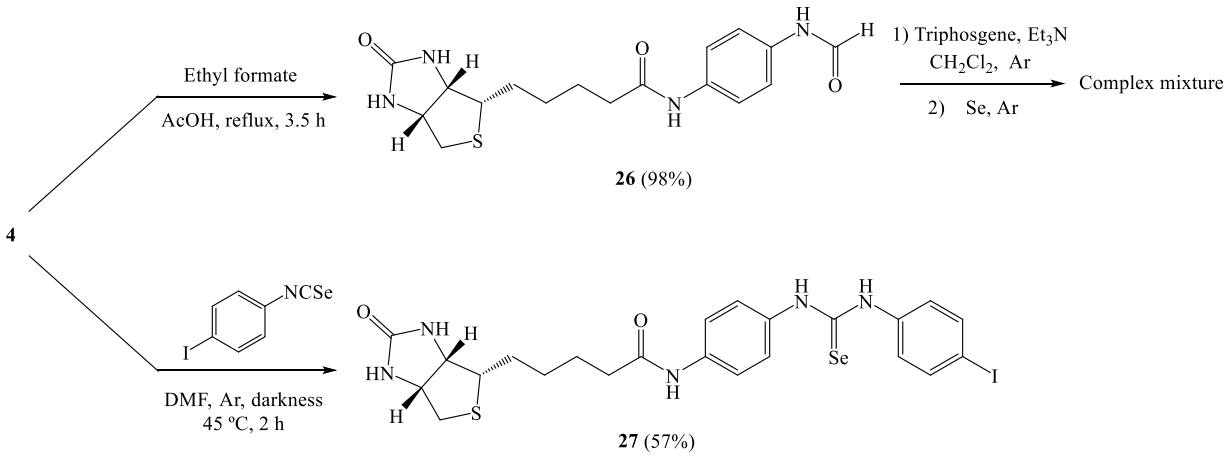

Scheme 6. Preparation of biotinylated selenourea **27**

In a similar fashion as described in Scheme 4, the analogous selenocyanates **28**, **29** and **30** were also prepared (Scheme 7). Again, the *N*-Boc protection proved to be not suitable for further derivatization. Enamine was selected again as the appropriate protecting group for accessing selenocyanate **30**, the building block for being conjugated with biotin. Resonances found at 101.7–104.6 ppm in ^{13}C-NMR spectra of compounds **28**–**30** confirmed the presence of the selenocyanato moiety in their structures.

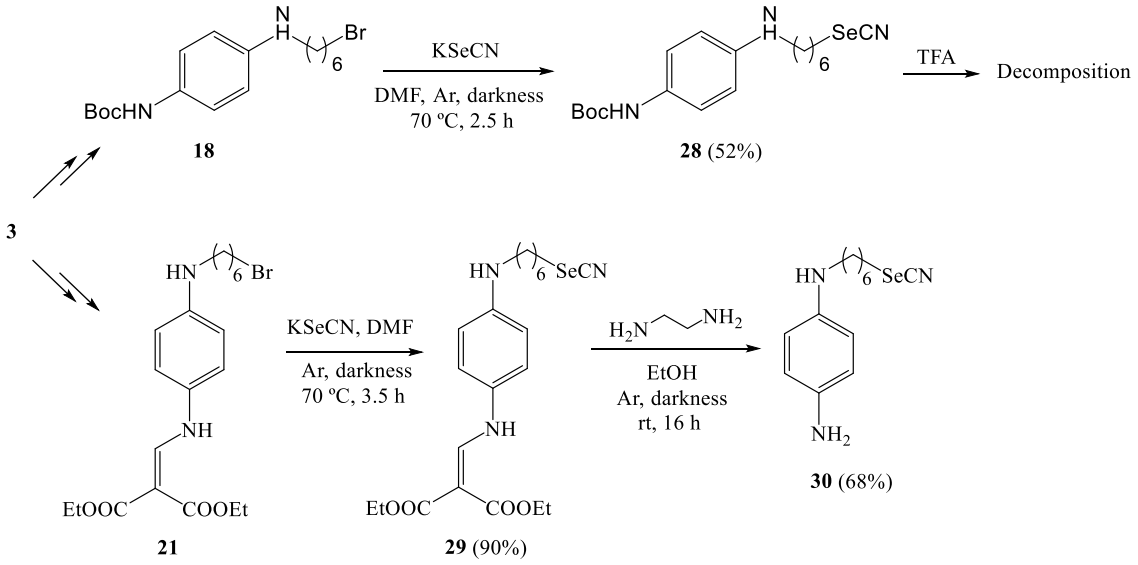

Scheme 7. Preparation of *N*-protected and *N*-unprotected selenocyanates **28**–**30**

Peptide coupling between biotin and *p*-amino selenocyanate **30** afforded biotinylated derivative **31** (Scheme 8), which could not be transformed into the corresponding dimeric diselenide, as a complex mixture was evidenced by TLC upon treatment with $NaBH_4$.

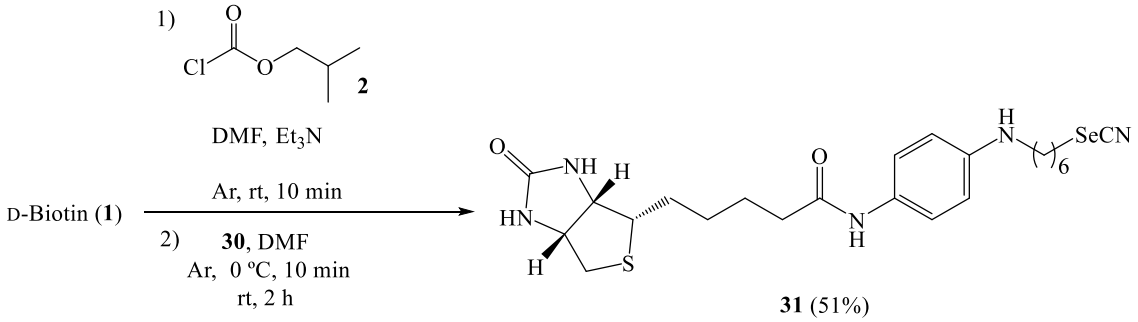

Scheme 8. Preparation biotinylated selenocyanate **31**

2.2. Biological assessment

2.2.1. In vitro *screening of antiproliferative activities*

Biotinylated derivatives **5**, **9**–**11**, **17**, **24**, **25**, **27** and **31** were screened against the following human tumour cell lines: A549 (non-small cell lung), HBL-100 (breast), HeLa (cervix), SW1573 (non-small cell lung), T-47D (breast) and WiDr (colon). BJ-

hTERT (human fibroblasts), as a non-tumour cell line was also included in the bioassay in order to determine the selectivity indexes (S.I.). Antiproliferative assays were carried out using minor modifications of the protocol from the US National Cancer Institute (NCI) [50].

The non-biotinylated counterparts **15**, **19**, **22**, **23**, **28**–**30** were also included in order to show the influence of the biotin residue. 5-Fluorouracil (5-FU) and cisplatin (CDDP) were also included as reference drugs.

2.2.1.1. SAR analysis for the antiproliferative assay

Antiproliferative activities (GI_{50}, μM) of biotinylated and non-biotinylated derivatives, together with the reference drugs are depicted in Table 1 (selected data) and Table S-1 (Supporting information file). A large range of activities can be found depending on the structural modifications accomplished.

Biotin was proved to be ineffective concerning antiproliferative properties (Table SI-1, compound **4**); thus, although biotin-derived isothiocyanate **5** showed moderate activities against the six tumour cell lines tested (GI_{50} = 18–38 μM), its transformation into free-OH thiosemicarbazones **9**–**11** and the *O*-acetylated counterpart **17** completely abolished activity (GI_{50} > 100 μM). This observation was further confirmed upon replacement of the biotin residue with a Boc-functionality (thiosemicarbazone **15**). In this case, moderate activities were obtained (GI_{50} = 16–25 μM).

Situation slightly improved upon replacement of the thiosemicarbazone scaffold with a thiocyanato motif (compound **24**, Table 1); in this case, a good antiproliferative activity against HeLa cell lines (GI_{50}= 6.3 μM) was obtained, and moderate for the rest (GI_{50} = 19–36 μM). Transformation into disulfide **25** was detrimental, with complete loss of activity. Nevertheless, the building blocks **22** (enamine-protected thiocyanate) and **23** (free NH_2), without the biotin residue, were endowed with improved activity compared to their biotinylated counterpart **24**, with low micromolar activities in most of the tested cell lines, and good selectivity (GI_{50} > 100 μM, BJ-hTert).

Activity was clearly increased when shifting to selenium analogues; thus, biotin-containing selenourea **27** exhibited moderate potency, unlike structurally related thiosemicarbazones **9**–**11**, devoid of any activities.

The most astonishing results were obtained by combination of biotin and selenocyanate scaffolds (Table 1). Prior to biotin conjugation, good activities were obtained for selenocyanate derivatives (**30** > **28** > **29**), particularly for the *N*-unprotected derivative **30**, with GI_{50} values ranging from high-nanomolar to submicromolar ranges, and excellent selectivities (S.I. 3500–433).

To our delight, conjugation of **30** with biotin afforded the lead compound (derivative **31**) in terms of potency (GI_{50}= 13–66 nM), and selectivities, reaching a S.I. as high as 7700 (Table 1). Interestingly, incorporation of biotin afforded up to a 7.6-fold increase in potency compared with the non-conjugated derivative **30** (only WiDr line was not improved). Moreover, activities of drug controls used herein were clearly overpassed by selenocyanate-biotin hybrid **31** (33–2130-fold for 5-FU, 37–1130-fold for CDDP); such controls exhibit quite reduced selectivities, a matter that can be responsible for their numerous and strong side-effects.

Table 1. Selected antiproliferative activities (GI_{50}, μM) against tumour and non-tumour cell lines[a,b]

Compound		**A549** (Lung)	**HBL-100** (Breast)	**HeLa** (Cervix)	**SW1573** (Lung)	**T-47D** (Breast)	**WiDr** (Colon)	**BJ-hTert** (Fibroblasts)	**S.I.**
Thiocyanate-NHBoc	**19**	14±2	16±3	19±4	16±3	18±6	29±7	n.t.	---
Thiocyanate-enamine	**22**	**2.7±0.6**	**3.5±1.6**	**3.4±0.6**	**1.8±0.6**	**4.9±1.4**	**5.0±0.6**	>100	>56 – >20
Thiocyanate-NH_2	**23**	**2.8±1.0**	**4.0±0.9**	**4.7±0.7**	**2.2±0.6**	17±4	15±3	>100	>36 – >6
Thiocyanate-biotin	**24**	29±11	19±1	6.3±1.7	22±2	34±4	36±7	n.t.	---
Disulfide-biotin	**25**	>100							
Selenourea-biotin	**27**	22±3	23±10	20±3	24±7	28±9	39±4		
Selenocyanate-NHBoc	**28**	**3.9±0.5**	**4.7±1.1**	**2.4±0.4**	**2.5±0.9**	**3.6±1.2**	**5.4±0.7**	>100	>42 – >19
Selenocyanate-enamine	**29**	**3.5±0.6**	12±2	13±3	**2.5±1.2**	16±4	18±6		>40 – > 2
Selenocyanate-NH_2	**30**	**0.21±0.00**	**0.18±0.01**	**0.086±0.019**	**0.13±0.03**	**0.026±0.011**	**0.12±0.06**	91±11	3500 – 433
Selenocyanate-biotin	**31**	**0.066±0.026**	**0.051±0.018**	**0.013±0.005**	**0.017±0.009**	**0.059±0.020**	**0.023±0.011**	>100	>7700 - >1515
5-FU		2.2±0.3	4.4±0.7	16±5	3.3±1.2	43±16	49±7	5.5±0.5	0.1–1.3
CDDP		4.9±0.2	1.9±0.2	1.8±0.5	2.7±0.4	17±3	26±4	14±2	0.5–7.4

[a]S.I.: Selectivity indextes, expressed as a range (S.I. = $G_{non\text{-}umour}/GI_{tumour}$); [b]Data in bold style represent GI_{50} values lower than 10 μM

2.2.2. Antiproliferative effects on sensitive/multidrug resistant cell lines

According to data depicted in Table 1, biotinylated selenocyanate **31** can clearly be considered as the lead compound, and therefore, a good candidate to further assays for the elucidation of its mode of action. The same assays were initially planned also for the non-biotinylated counterpart **30**; nevertheless, its reduced solubility under the assays conditions, precluded its evaluation.

An important issue to be considered when developing new anticancer drugs is their behaviour towards resistant cell lines. Multidrug resistance (MDR) is indeed one of the major problems and challenges to be solved in chemotherapies, as it accounts for 90% of deaths [51]. Although numerous mechanisms responsible for the development of MDR are currently known, special attention should be given to ATP-binding cassette (ABC) superfamily of transporters, among which P-glycoprotein efflux pump (P-gp) is overexpressed in numerous tumours [8]; as a result, cytotoxic chemotherapeutic agents are extruded from the cells, leading to failure of the anticancer therapy. Moreover, the faster the cancer cells can adapt to unfavourable situations (e.g. through metabolic pathways, redox changes, autophagy, increased capacity of repairing DNA, etc.) provoked by the chemotherapeutic agents, the higher resistance will be observed [52].

In this context, the effects of **31** on cell growth were studied in NCI-H460 (lung), NCI-H460/R (lung, resistant cell line), and MRC-5 cells (fibroblasts, non-tumour). Table 2 summarizes the GI_{50} values obtained by the sulforhodamine B (SRB) assay. Although the potency of **31** against the lung cell lines used in Table 2 is sensibly lower that against the six cell lines depicted in Table 1, the possibility of analyzing the effects on a sensitive/resistant couple deserves attention.

Biotinylated selenocyanate **31** inhibited the growth of drug-sensitive cancer cells, with remarkable selectivity towards cancer cells.

Furthermore, considerable difference in sensitivity between sensitive and MDR cells was also noticed. Specifically, as indicated in Table 2, NCI-H460/R cells (which overexpress P-glycoprotein) were approximately 10-fold more resistant to **31** compared to NCI-H460.

Table 2. GI_{50} values (μM) for the antiproliferative activity of **31** in NCI-H460, NCI-H460/R, and MRC-5 cells					
Compound	**NCI-H460** (Lung)	**NCI-H460/R** (Lung)	**MRC-5** (Fibroblasts) (non-tumour)	**S.I.**	**Resistance factor** (NCI-H460/R / NCI-H460)
31	11.1±1.29	116.6±1.46	136.1±1.26	12	10.5

We next addressed the interaction of **31** with P-glycoprotein. The potential of **31** (10 and 100 μM) to modulate the P-glycoprotein function was evaluated by rhodamine 123 accumulation assay and was compared to TQ, a third-generation P-glycoprotein inhibitor (Fig. 2). Treatment with 50 nM TQ successfully inhibited activity of this efflux pump in NCI-H460/R cells, resulting in the accumulation of rhodamine 123 similar to NCI-H460 cells. However, **31** displayed P-glycoprotein substrate properties which was evident by dose-dependent competitive reduction in cellular efflux of fluorescent rhodamine 123, a substrate of P-glycoprotein. Namely, the addition of 10 μM **31** did not modulate the P-glycoprotein function, while 100 μM treatment increased rhodamine accumulation by approximately 50%.

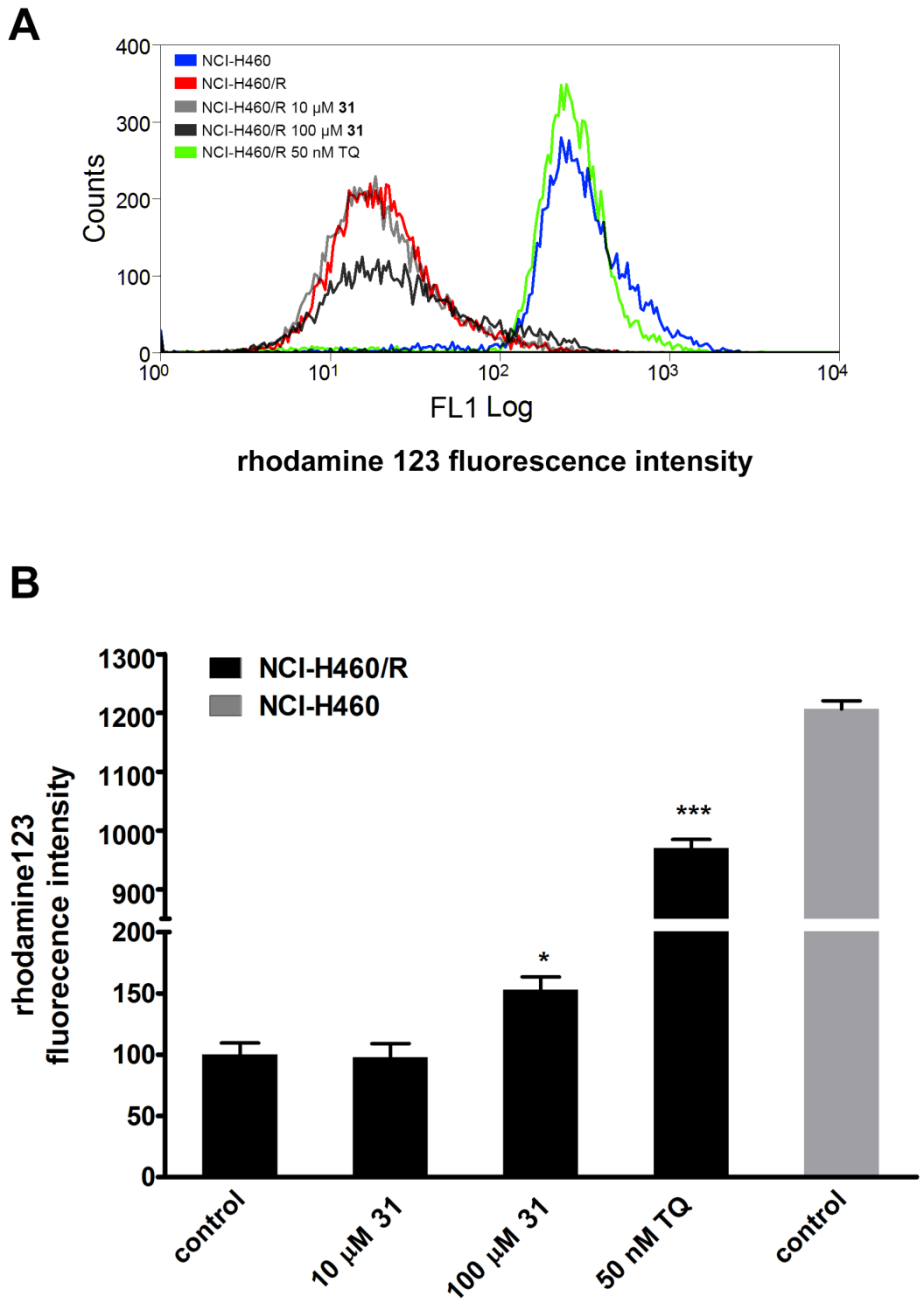

Figure 2. Effect of **31** on P-gp activity. (A) Flow-cytometry assay for the accumulation of rhodamine 123 in in NCI-H460/R cells treated with **31**. (B) Rhodamine 123 fluorescence in NCI-H460/R cells treated with **31**. Statistical significant difference (ANOVA test) compared to NCI-H460/R control cells: $p < 0.05$ (*), $p < 0.001$ (***).

To evaluate if the activity of P-glycoprotein is responsible for the resistance of NCI-H460/R cells to **31**, the compound's effects on cell growth inhibition in combination with TQ was tested by the sulforhodamine B assay (Figure 3). TQ, without effects on the growth of cells, improved **31** efficacy in resistant cells. Specifically, the GI_{50} value of **31** in NCI-H460/R was lowered from 116.6 µM to 33.5 µM upon the

addition of TQ. The cell growth inhibition profiles of **31** in NCI-H460/R cells with or without the addition of TQ are shown in Figure 3, and compared to the cell growth inhibition profile of **31** in sensitive parental cell line.

Therefore, the observed resistance of NCI-H460/R cells to **31** is likely a result of its lower cellular accumulation due to P-glycoprotein activity.

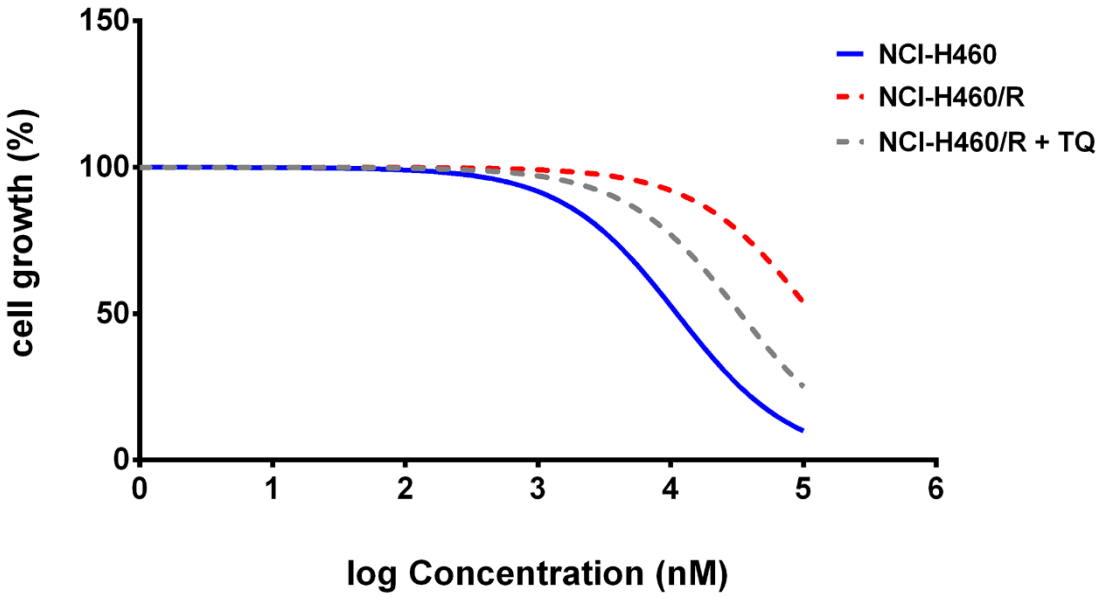

Figure 3. Effect of administration of TQ + **31** against NCI-H460/R cells (nonlinear regression)

2.2.3. Cell death analysis (Annexin-V assay)

The effect of the compound on cell death induction was then analysed. Flow-cytometric analysis of cell death showed that **31** considerably increased a number of apoptotic NCI-H460 cells. The amount of NCI-H460 cells in early apoptosis (AV+ PI−) increased from 0.3% in control (untreated cells) to 12% for cells treated with **31** (10 μM, Fig. 4A and B). Viable (AV− PI−) and necrotic (AV− PI+) cells are also depicted in Figure 4A and B. The number of cells in late apoptosis (AV+ PI+) increased from 0.3% in control to 24% for cells treated with compound **31** (Fig. 4). Conventional chemotherapeutic DOX (doxorubicin) was used as a positive control for inducing cell death.

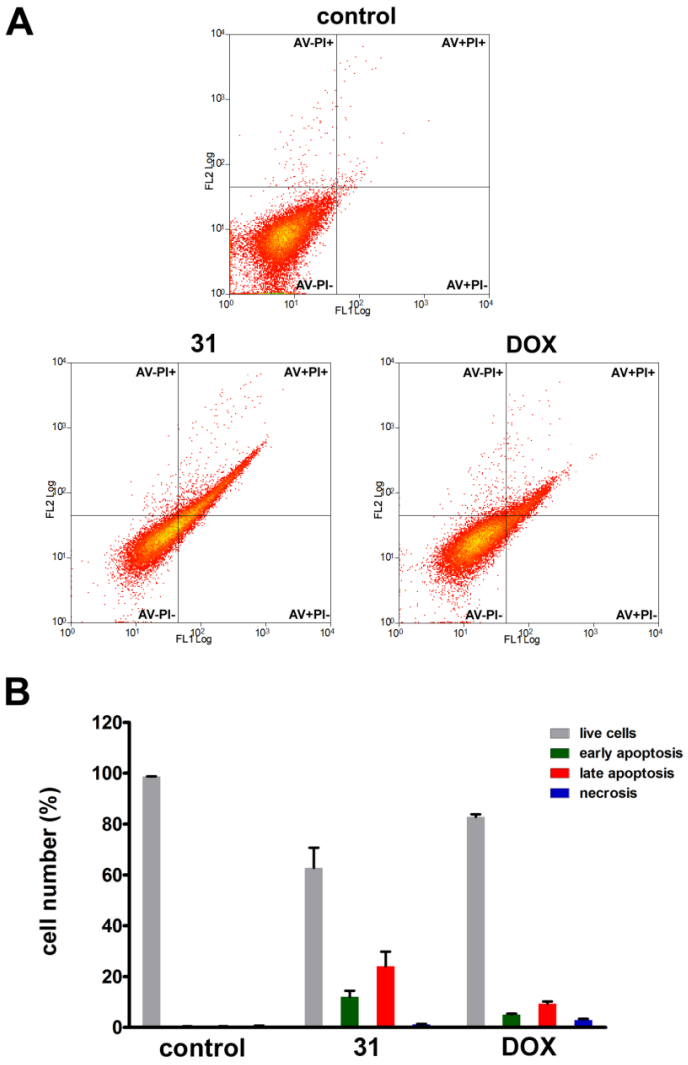

Figure 4. Annexin-V/PI staining assay on NCI-H460 cells treated with **31** (10 µM).

2.2.4. Analysis of mitochondrial transmembrane potential

During apoptosis, outer and inner mitochondrial membranes increase their permeability [53]; for that reason, mitochondrial membrane potential can be considered as an early marker for apoptosis. Tetramethylrhodamine (TMRE) staining was used to evaluate the effect of **31** on the mitochondrial membrane potential in NCI-H460 cells. Depolarization of mitochondrial membrane was detected by flow cytometry in cells treated with 10 µM **31** after 48 h (Fig. 5A), which corresponded with apoptosis observed in this cell line under the same conditions (Fig. 4). Carbonyl cyanide *m*-chlorophenyl hydrazone (CCCP), a mitochondrial uncoupling agent was used as a positive control for dissipation of mitochondrial membrane potential.

The inability of depolarized mitochondria to sequester TMRE in **31**-treated NCI-H460 cells was also visualized by fluorescent microscopy (Fig. 5B).

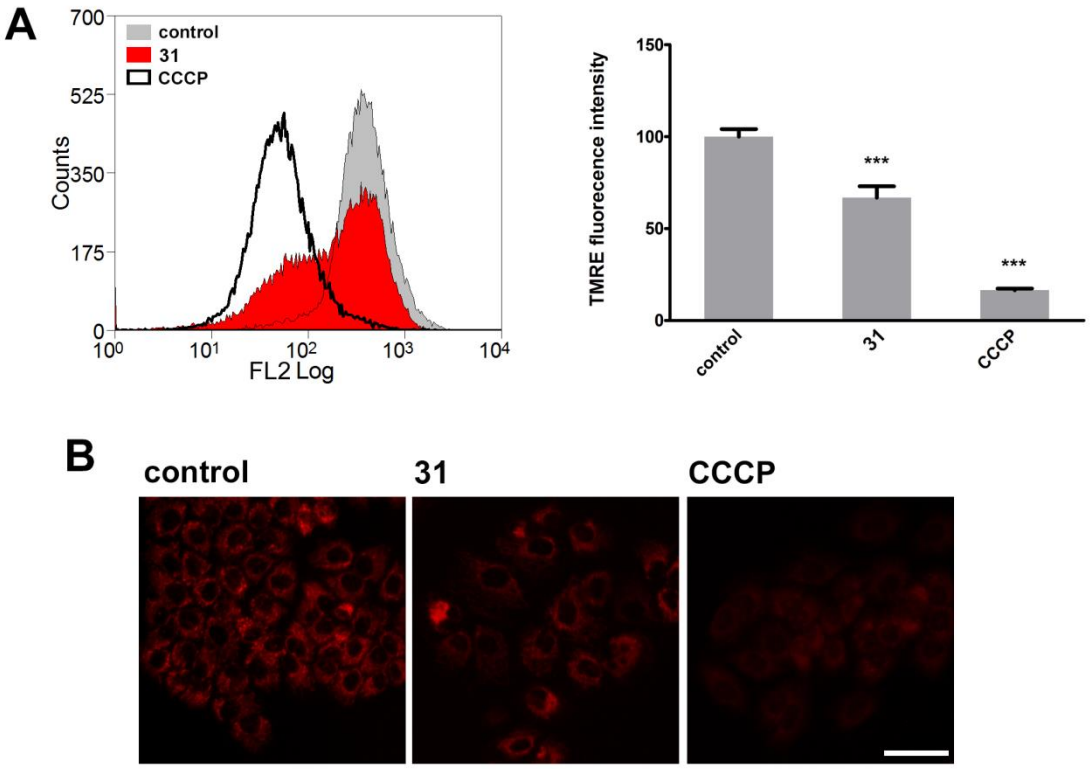

Figure 5. Mitochondrial transmembrane potential changes provoked by **31**. TMRE staining was used in the treatment of NCI-H460 cells with **31** (10 µM, 48 h). (A) Flow-cytometric profiles of TMRE-stained cells after treatments with **31** and CCCP (left panel). Fluorescence intensity of TMRE (arbitrary units) of NCI-H460-treated cells (right panel). Statistical significant difference (ANOVA test) compared to control cells: $p < 0.001$ (***). (B) Fluorescence microscopy on NCI-H460-treated cells

2.2.5. Continuous Live-Cell Imaging

To study in more detail the phenotypic effects of compound **31**, we used label-free continuous live-cell imaging microscopy. With this technique, we monitored (every 5 minutes) at single cell level the effects of the exposure to **31** (100 nM) for 20 h on the lung cancer cells SW1573. As a result, cytostatic effects were induced by **31** on treated cells (Supplementary material, videos S1 and S2). Untreated cells moved freely and divided, almost doubling the population at the end of the experiment. In contrast, the number of treated cells remained constant and no cell division was observed. Cell morphology experienced changes as time progressed, distinguishing several apoptotic

hallmarks. This observation is consistent with the results obtained in the cell death analysis.

2.2.6. Measurement of the inhibition of histones deacetylases (HDACs)

Histones are small metalloproteins that bind DNA strands to furnish chromatin, whose post-translational modifications (methylation, phosphorylation, acetylation, deacetylation) regulates gene expression. In particular, acetylation and deacetylation of histones depend on the enzymes histone acetyltransferases (HATs) and deacetylases (HDACs) [54]. The latter enzymes are overexpressed in numerous tumours, yielding aberrant deacetylation in the terminal lysine units of histones. As a result, a more compact chromatine is obtained, causing the repression of certain genes involved in the control of cell growth and death, and thus, allowing the development of tumour cells [55].

Therefore, inhibition of HDACs is currently considered as an attractive therapeutic target in the development of new anticancer agents. The most common family of such inhibitors is comprised of hydroxamates, which chelate the Zn^{2+} ion of the enzyme active site. In this context, SAHA (suberoylanilide hydroxamic acid, Vorinostat®) was approved by FDA against cutaneous T cell lymphoma [56].

SelSA, a selenocyanate structurally related to **30** was reported to be a good inhibitor of HDAC-6 [30]. For that purpose, derivatives **30** and **31** were also tested as potential inhibitors of HDACs to determine if such activity also contributes to their antiproliferative mechanism.

Unfortunately, derivatives **30** and **31** were found to be considerably weaker inhibitors than SAHA (IC_{50}= 0.27 ± 0.08 μM) and SelSA (Figure 6), and although inhibition of HDACs can not be ruled out, it would be a minor contribution to their antiproliferative mode of action. The lower activity compared to SAHA is likely due to the monodentate coordination to Zn, which will be weaker compared to the bidentate coordination of SAHA. Furthermore, SAHA benefits from a hydrogen bond interaction between its PhNHCO- group and the enzyme active site cavity entrance, whereas this type of interaction is not present in **30**, **31**, due to the absence of such amide moiety.

Moreover, the behaviour of both compounds in a dose-dependent inhibition experiment (Figure 6) could suggest a weak interaction that does not involve binding in the enzyme active site.

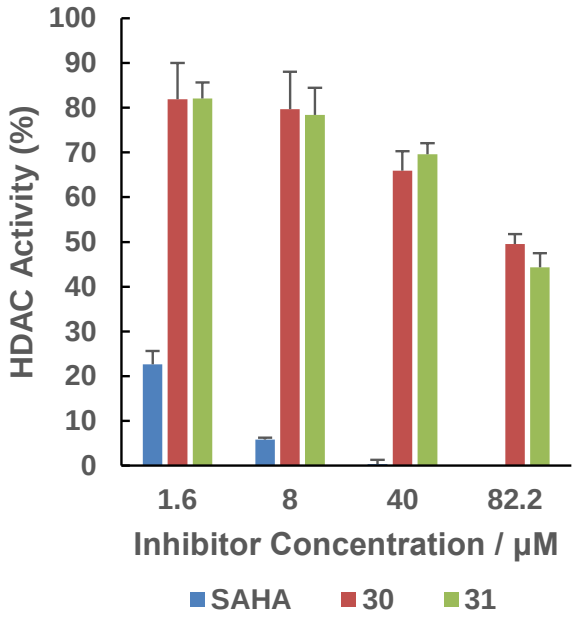

Figure 6. HDAC activity at various inhibitor concentrations (**30**, **31**). SAHA was used as a positive control

3. Conclusions

In conclusion, conjugation of biotin with organochalcogen scaffolds for the development of antiproliferative agents was found to be highly dependent on the nature of the organochalcogen motif. This approach turned out to be particularly effective in the case of selenocyanates, providing very strong and selective antiproliferative agents, with activities reaching the nM range in six out of the seven human tumour cell lines tested. Apoptosis and depolarization of the mitochondria membrane were found to be involved in the mode of action of biotinylated selenocyanates Prior to the apoptotic events, cytostatic effects were observed against SW1573 cells using label-free cell-living imaging; therefore, tumour cell division was prevented.

Moreover, as a way of avoiding P-gp-mediated chemoresistance, co-administration with tariquidar turned out to be a valid alternative.

Therefore, biotinylated selenocyanate **31** could be considered as an attractive lead compound in the development of new families of chemotherapeutic agents against cancer.

4. Experimental section

4.1. Materials and methods

4.1.1. General procedures

The same general procedures concerning chromatography, NMR spectroscopy and MS spectrometry as reported previously [57] were used.

4.1.2. Antiproliferative activities

The *in vitro* antiproliferative activity against the panel of 6 tumour cell lines, and the non-human line (BJ-hTert) was assayed using minor modifications of the protocol of the US National Cancer Institute (NCI) [50].

For the assays against the lines NCI-H460 and NCI-H460/R, the conditions reported previously were used [57].

4.1.3. Sulforhodamine B assay

The same conditions as reported previously [57] were used; compound **31** was tested in a 1 nM – 100 μM concentration range.

4.1.4. Rhodamine 123 accumulation assay

The same conditions as reported previously [57] were used; NCI-H460/R cells were treated with 10 μM and 100 μM **31**.

4.1.5. Cell death analysis by flow cytometry

The same conditions as reported previously [57] were used; NCI-H460 cells were incubated at a density of 200,000 cells/well. The cells were treated with 10 μM **31** for 48 h.

4.1.6. Mitochondrial transmembrane potential analysis

The effect of **31** on mitochondrial membrane potential was analysed using the cell-permeant dye TMRE [58]. NCI-H460 cells were seeded in 6-well tissue culture plate (200,000 cells/well), incubated overnight, and treated with 10 µM **31** for 48 h. As a positive control, cells were also treated with 10 µM CCCP for 30 min prior to TMRE staining. Next, the cells were stained with 500 nM TMRE for 30 min at 37 °C in the dark.

To visualize the effect of **31** on mitochondrial membrane potential, the cells were imaged live on ZOE Fluorescent Cell Imager (Bio-Rad Laboratories, Hercules, CA, USA), 20× objective. TMRE fluorescence was also quantified on a CyFlow Space flow cytometer (Partec, Münster, Germany) by measuring fluorescence emission in FL2 channel. At least 20,000 events were recorded per each sample.

4.1.7. Continuous live-cell imaging

The imaging platform microscope CX-A (Nanolive SA, Lausanne, Switzerland) was used, under the conditions previously reported [59, 60]. Compound **31** was used at a 100 nM concentration, and images were acquired every 5 min for 20 h.

4.1.8. Inhibition of HDACs

The same conditions as previously reported were used [61]; compounds **30** and **31** were tested in a 0.512 nM–82.2 µM range.

4.2. Chemistry

*4-[4'-(Biotinylamino)phenyl)]-1-(4-hydroxybenzylidene)-3-thiosemicarbazone (**9**).* To a solution of isothiocyanate **5** (85.1 mg, 0.23 mmol) in CH_2Cl_2 (7.5 mL) was added hydrazine monohydrate (17 µL, 0.34 mmol, 1.5 equiv.), and the resulting solution was kept stirring at rt in the darkness for 17 h; after that, it was concentrated to dryness.

To the crude reaction dissolved in EtOH (9 mL) was added *p*-hydroxybenzaldehyde (59.1 mg, 0.48 mmol, 2.1 equiv.), and the mixture was refluxed in the darkness for 3 h. After that, 40 mL EtOH was added, and the corresponding mixture was centrifuged in a Falcon® tube at 3,000 rpm for 2 min; the precipitated was washed with 35 mL EtOH and centrifuged again under the same conditions. The supernatant was decanted, and the

solid was collected with CH_2Cl_2 and evaporated to give pure **9** as a pale green solid. Yield: 78.8 mg (67%). Mp: 232–240 ºC (dec.); $[\alpha]_D^{23}$ = +28 (*c* 0.81, DMSO); ^{1}H-NMR (300 MHz, $(CD_3)_2SO$) δ 11.59 (s, 1H, NH), 9.91 (s, 1H, OH), 8.05 (s, 1H, CH=N), 7.72 (m, 2H, Ar-H), 7.50 (m, 4H, Ar-H), 6.80 (m, 2H, Ar-H), 6.45 (s, 1H, NH biotin), 6.37 (s, 1H, NH biotin), 4.31 (m, 1H, CH-N), 4.15 (m, 1H, CH-N), 3.13 (m, 1H, CH-S), 2.82 (dd, 1H, $J_{H,H}$ = 5.0 Hz, $J_{H,H}$ = 12.4 Hz, H-C*H*-S), 2.58 (d, 1H, $J_{H,H}$ = 12.4 Hz, H-C*H*-S), 2.31 (t, 2H, $J_{H,H}$ = 7.2 Hz, CH_2), 1.50 (m, 6H, CH_2) ppm; ^{13}C-NMR (75.5 MHz, $(CD_3)_2SO$) δ 175.5 (C=S), 171.0 (C=O), 162.7 (C=O), 159.4 (Ar-C-OH), 143.1 (C=N), 136.5, 134.1, 129.4, 126.2, 125.0, 118.6, 115.5 (Ar-C), 61.0 (NH-CH), 59.2 (NH-CH), 55.4 (S-CH), 40.2 (SCH_2), 36.2, 28.2, 28.1, 25.1 (CH_2) ppm; HRESI-MS calcd. for $C_{24}H_{29}N_6O_3S_2$ ($[M+H]^+$): 513.1737, found: 513.1733.

4-[4'-(Biotinylamino)phenyl)]-1-(3,4-dihydroxybenzylidene)-3-thiosemicarbazone ***(10)****.* To a solution of isothiocyanate **5** (63.8 mg, 0.17 mmol) in CH_2Cl_2 (5 mL) was added hydrazine monohydrate (9 µL, 0.17 mmol, 1.0 equiv.), and the resulting solution was stirred at rt in the darkness for 6 h. After that, more hydrazine was added (9 µL, 0.18 mmol, 1.0 equiv.), and kept stirring for further 16 h. Then, the mixture was concentrated to dryness the residue was dissolved in EtOH (5 mL), and 3,4-dihydroxybenzaldehyde (46.1 mg, 0.33 mmol, 1.9 equiv.) was added; reaction was refluxed in the darkness for 2 h. After that, EtOH (20 mL) was added and the mixture was centrifuged in a Falcon® tube at 3,000 rpm for 2 min. The precipitate was washed with EtOH (15 mL) and further congregated under the same conditions. The supernatant was decanted and the precipitate was collected with CH_2Cl_2 and concentrated to dryness to give **5** as a pale yellow solid. Yield: 49.8 mg (56%). Mp: 246–250 ºC (dec.); $[\alpha]_D^{22}$ = +34 (*c* 0.69, DMSO); ^{1}H-NMR (300 MHz, $(CD_3)_2SO$) δ 11.55 (s, 1H, NH), 9.90 (s, 1H, OH), 9.86 (s, 1H, OH), 9.53 (s, 1H, NH), 9.00 (s, 1H, NH), 7.98 (s, 1H, CH=N), 7.50 (m, 4H, Ar-H), 7.31 (d, 1H, $J_{2,6}$ = 1.6 Hz, H-2 catechol), 7.10 (dd, 1H, $J_{2,6}$ = 1.6 Hz, $J_{5,6}$ = 8.6 Hz, H-6 catechol), 6.77 (d, 1H, $J_{5,6}$ = 8.6 Hz, H-5 catechol), 6.45 (s, 1H, NH biotin), 6.37 (s, 1H, NH biotin), 4.31 (m, 1H, CH-N), 4.14 (m, 1H, CH-N), 3.13 (m, 1H, CH-S), 2.83 (dd, 1H, $J_{H,H}$= 5.1 Hz, $J_{H,H}$ = 13.1 Hz, H-C*H*-S), 2.58 (d, 1H, $J_{H,H}$ = 13.1 Hz, H-C*H*-S), 2.31 (t, 2H, $J_{H,H}$= 7.0 Hz, CH_2), 1.50 (m, 6H, $3CH_2$) ppm; ^{13}C-NMR (75.5 MHz, $(CD_3)_2SO$) δ 175.9 (C=S), 171.6 (C=O), 163.2 (C=O), 148.4 (Ar-C-OH), 146.0 (Ar-C-OH), 144.1 (C=N), 137.0, 134.6, 126.5, 125.9, 121.1, 119.1, 115.9, 114.5 (Ar-C), 61.5 (NH-CH), 59.7 (NH-CH), 55.9 (S-CH), 40.3 (S-CH_2), 36.7 (CH_2), 28.7, 28.5, 25.6

(CH_2) ppm; HRESI-MS calcd. for $C_{24}H_{28}N_6NaO_4S_2$ ($[M+Na]^+$): 551.1506, found: 551.1497.

4-[4'-(Biotinylamino)phenyl)]-1-(3,4,5-trihydroxybenzylidene)-3-thiosemicarbazone ***(11)***. To a solution of isothiocyanate **5** (85.1 mg, 0.23 mmol) in CH_2Cl_2 (7.5 mL) was added hydrazine monohydrate (17 µL, 0.35 mmol, 1.5 equiv.) and was kept stirring at rt in the darkness for 17 h. After that, the mixture was concentrated to dryness the residue was dissolved in EtOH (8 mL) and 3,4,5-trihydroxybenzaldehyde (49.6 mg, 0,32 mmol, 1.4 equiv.); reaction was heated at 50 ºC in the darkness under Ar for 80 min.

Then, EtOH (30 mL) was added and the mixture was centrifuged in a Falcon® tube at 3,000 rpm for 2 min. The precipitate was washed with EtOH (20 mL) and further centrifuged under the same conditions. The supernatant was decanted and the precipitate was collected with CH_2Cl_2 and concentrated to dryness to give **11** as a pale orange solid. Yield: 77.1 mg (62%). Mp: 204–210 ºC (dec.); $[\alpha]_D^{24}$ = +27 (*c* 0.76, DMSO); ^{1}H-NMR (300 MHz, $(CD_3)_2SO$) δ 11.51 (s, 1H, NH), 9.88 (s, 1H, OH), 9.82 (s, 1H, OH), 9.01 (s, 1H, NH), 8.69 (s, 1H, OH), 7.90 (s, 1H, CH=N), 7.49 (m, 4H, Ar-H), 6.77 (s, 2H, Ar-H), 6.44 (s, 1H, NH biotin), 6.33 (s, 1H, NH biotin), 4.31 (m, 1H, CH-N), 4.13 (m, 1H, CH-N), 3.12 (m, 1H, CH-S), 2.83 (dd, 1H, $J_{H,H}$ = 5.0 Hz, $J_{H,H}$ = 12.5 Hz, H-C*H*-S), 2.57 (d, 1H, $J_{H,H}$ = 12.5 Hz, H-C*H*-S), 2.31 (m, 2H, CH_2), 1.50 (m, 6H, $3CH_2$) ppm; ^{13}C-NMR (75.5 MHz, $(CD_3)_2SO$) δ 175.8 (C=S), 171.5 (C=O), 163.2 (C=O), 146.6 (Ar-C-OH), 144.5 (C=N), 136.9 (Ar-C-OH), 136.4, 134.5, 126.3, 124.7, 119.1, 107.4 (Ar-C), 61.5 (NH-CH), 59.6 (NH-CH), 55.9 (S-CH), 40.3 (S-CH_2), 36.6, 28.7, 28.5, 25.6 (CH_2) ppm; HRESI-MS calcd. for $C_{24}H_{29}N_6O_5S_2$ ($[M+H]^+$): 545.1635, found: 545.1628.

*4-[4'-(*terc*-Butoxycarbonylamino)phenyl]-3-thiosemicarbazide* ***(14)***. To a solution of isothiocyanate **13** (150.4 mg, 0.60 mmol) in CH_2Cl_2 (10 mL) was added hydrazine hydrate (59 µL, 1.20 mmol, 2.0 equiv.); just after the addition, a white precipitate was formed, which was filtered, and dried to give pure **14**. Yield: 149.5 mg (88%). Mp: 191–197 ºC; ^{1}H-NMR (300 MHz, $(CD_3)_2SO$) δ 9.50 (s, 1H, NH), 9.26 (s, 1H, s, NH), 9.00 (s, 1H, NH), 7.39 (m, 4H, Ar-H), 4.73 (s, 2H, NH_2), 1.47 (s, 9H, $C(CH_3)_3$) ppm; ^{13}C-NMR (75.5 MHz, $(CD_3)_2SO$) δ 180.0 (C=S), 153.3 (C=O), 136.4, 134.0, 124.8,

118.3 (Ar-C), 79.3 ($C(CH_3)_3$), 28.6 (C(CH_3)$_3$) ppm; HRESI-MS: calcd. for $C_{12}H_{18}N_4NaO_2S$ ($[M+Na]^+$): 305.1043, found: 305.1042.

*4-[4'-(*terc-*Butoxycarbonylamino)phenyl]-1-(3,4-dihydroxybenzylidene)-3-thiosemicarbazone (**15**).* A solution of thiosemicarbazide **14** (113.9 mg, 0.40 mmol) and 3,4-dihydroxybenzaldehyde (111.7 mg, 0.81 mmol, 2.0 equiv.) in EtOH (7 mL) was refluxed in the darkness under Ar for 1 h. Then, it was concentrated to dryness, and the residue was purified by column chromatography (cyclohexane → 2:1 Et_2O–cyclohexane) to give **15** as a white solid. Yield: 59.7 mg (38%). Mp: 191–197 ºC. ^{1}H-NMR (300 MHz, $(CD_3)_2SO$) δ 11.52 (s, 1H, NH), 9.83 (s, 1H, OH), 9.51 (s, 1H, NH), 9.33 (s, 1H, OH), 8.99 (s, 1H, NH), 7.98 (s, 1H, CH=N), 7.40 (s, 4H, Ar-H), 7.31 (d, 1H, $J_{H,H}$ = 1.9 Hz, H-2 catechol), 7.09 (dd, 1H, $J_{H,H}$ = 8.2 Hz, $J_{H,H}$ = 1.9 Hz, H-6 catechol), 6.78 (d, 1H, $J_{H,H}$ = 8.1 Hz, H-5 catechol), 1.48 (s, 9H, C(CH_3)$_3$) ppm; ^{13}C-NMR (75.5 MHz, $(CD_3)_2SO$) δ 175.5 (C=S), 152.8 (C=O), 147.9, 145.6 (Ar-C), 143.6 (C=N), 136.8, 126.2, 125.5, 120.6, 117.7, 115.5, 114.1 (Ar-C), 79.0 ($C(CH_3)_3$, 28.2 (C(CH_3)$_3$) ppm; HRESI-MS calcd. for $C_{19}H_{22}N_4NaO_4S$ ($[M+Na]^+$): 425.1254, found: 425.1248.

*4-[4'-(Biotinylamino)phenyl)]-1-(3,4-diacetoxybenzylidene)-3-thiosemicarbazone (**17**).* To a solution of isothiocyanate **5** (69.9 mg, 0.19 mmol) in CH_2Cl_2 (6.5 mmol) was added hydrazine hydrate (14 µL, 0.29 mmol, 1.5 equiv.), and the corresponding solution was kept stirring at rt in the darkness under Ar for 3.5 h. After that, it was concentrated to dryness and the crude thiosemicarbazide was dissolved in EtOH (6 mL), and 3,4-diacetoxybenzaldehyde (67.6 mg, 0.38 mmol, 2.0 equiv.) was added. The mixture was refluxed in the darkness under Ar for 3.5 h. A precipitate was formed, that was suspended in EtOH (15 mL) and centrifuged in a Falcon® tube at 3,000 rpm for 2 min. The supernatant was decanted and the precipitate was collected with CH_2Cl_2 and evaporated to dryness to give pure **17** as a pale yellow solid. Yield: 91.2 mg (78%). Mp: 216–224 ºC; $[\alpha]_D^{26}$ = +26 (*c* 1.02, DMSO); ^{1}H-NMR **(**300 MHz, $(CD_3)_2SO$) δ 11.84 (s, 1H, NH), 10.11 (s, 1H, NH), 9.92 (s, 1H, NH), 8.13 (s, 1H, CH=N), 7.97 (d, 1H, $J_{H,H}$ = 1.7 Hz, H-2 catechol), 7.74 (dd, 1H, $J_{H,H}$ = 8.4 Hz, $J_{H,H}$ = 1.7 Hz, H-6 catechol), 7.59 (m, 2H, Ar-H), 7.40 (m, 2H, Ar-H), 7.33 (d, 1H, d, *J* = 8.4 Hz, H-5 catechol), 6.46 (s,

1H, NH biotin), 6.37 (s, 1H, NH biotin), 4.32 (m, 1H, CH-N), 4.16 (m, 1H, CH-N), 3.14 (m, 1H, CH-S), 2.84 (dd, 1H, $J_{H,H}$ = 4.9 Hz, $J_{H,H}$ = 12.4 Hz, H-C*H*-S), 2.57 (d, 1H, $J_{H,H}$ = 12.5 Hz, H-C*H*-S), 2.30 (m, 8H, CH_2, 2OAc), 1.52 (m, 6H, $3CH_2$) ppm; ^{13}C-NMR (75.5 MHz, $(CD_3)_2SO$) δ 176.8 (C=S), 171.5 (C=O), 168.7 (C=O, Ac), 168.6 (C=O, Ac), 163.2 (C=O), 143.6 (Ar-C-O), 142.9 (C=N), 141.4 (Ar-C-O), 137.4, 134.0, 133.4, 127.2, 127.0, 124.3, 122.2, 119.1 (Ar-C), 61.5 (N-CH), 59.7 (N-CH), 55.9 (S-CH), 40.3 (S-CH_2), 36.7, 28.7, 28.6, 25.6 (CH_2), 20.9, 20.8 (OAc) ppm; HRESI-MS calcd. for $C_{28}H_{33}N_6O_6S_2$ ($[M+H]^+$): 613.1898, found: 613.1889.

tert-*Butyl {4-[(6'-thiocyanatohexyl)amino]phenyl}carbamate (**19**)*. A solution of *N*-Boc-protected *p*-phenylenediamine **12** (50.6 mg, 0.24 mmol), 1,6-dibromohexane (115 µL, 0.72 mmol, 3.0 equiv.) and KOH (30.7 mg, 0.52 mmol, 2.2 equiv.) was stirred at rt for 1 h. After that, it was concentrated to dryness and the residue was purified by column chromatography (cyclohexane → 1:4 EtOAc–cyclohexane) to give the corresponding 6-bromo derivative **18** (49.2 mg, 55%). A solution of **18** (213.6 mg, 0.58 mmol) and KSCN (173.5 mg, 1.78 mmol, 3.0 equiv.) in DMF (5 mL) was heated at 70 ºC under Ar for 2.5 h. Then, it was concentrated to dryness, and the residue was purified by column chromatography (cyclohexane → 1:4 EtOAc–cyclohexane) to give **19** as a light brown syrup. Yield: 145.7 mg (72%). ^{1}H-NMR (300 MHz, $CDCl_3$) δ 6.92 (m, 2H, Ar-H), 6.66 (m, 2H, Ar-H), 3.58 (s, 2H, NH), 3.54 (t, 2H, $J_{H,H}$ = 7.4 Hz, CH_2), 2.91 (t, 2H, $J_{H,H}$ = 7.4 Hz, CH_2), 1.79 (m, 2H, CH_2), 1.42 (m, 6H, $3CH_2$), 1.40 (s, 9H, $C(CH_3)_3$) ppm; ^{13}C-NMR (75.5 MHz, $CDCl_3$) δ 155.4 (C=O), 144.1, 134.0, 128.4, 115.7 (Ar-C), 112.5 (SCN), 79.8 ($C(CH_3)_3$), 49.9, 34.1, 29.9, 29.8 (CH_2), 28.5 ($C(CH_3)_3$), 27.7 (CH_2), 26.1 (CH_2) ppm; HRESI-MS calcd. for $C_{18}H_{28}N_3O_2S$ ($[M+H]^+$): 350.1897, found: 350.1894.

*Diethyl 2-{[(4'-((6''-bromohexyl)amino)phenyl)amino]methylene}malonate (**21**)*. A solution of enamine **20** (201.5 mg, 0.72 mmol) and K_2CO_3 (200.0 mg, 1.45 mmol, 2.0 equiv.) in DMF (1.5 mL) was stirred at rt for 40 min; after that, 1,6-dibromohexane (440 µL, 2.86 mmol, 4.0 equiv.) was added, and the mixture was stirred at rt under Ar for 4.5 h. Then, it was concentrated to dryness and the residue was purified by column chromatography (cyclohexane → 1:2 Et_2O–cyclohexane) to give **21** as a yellow solid. Yield: 139.6 mg (44%). Mp: 67–77 ºC; ^{1}H-NMR (300 MHz, $CDCl_3$) δ 10.95 (d, 1H, $J_{H,H}$= 14.1 Hz, Ar-N*H*-CH=), 8.40 (d, 1H, $J_{H,H}$= 14.1 Hz, Ar-NH-C*H*=), 6.99 (m, 2H,

Ar-H), 6.65 (m, 2H, Ar-H), 4.49 (s, 1H, Ar-NH), 4.29 (q, 2H, $J_{H,H}$ = 7.4 Hz, CH_2-CH_3), 4.22 (q, 2H, $J_{H,H}$ = 7.1 Hz, CH_2-CH_3), 3.41 (t, 2H, $J_{H,H}$ = 6.7 Hz, CH_2-Br), 3.11 (t, 2H, $J_{H,H}$ = 7.0 Hz, CH_2-N), 1.87 (m, 2H, CH_2), 1.65 (m, 2H, CH_2), 1.46 (m, 4H, 2CH_2), 1.37 (t, 3H, $J_{H,H}$= 7.1 Hz, CH_2-CH_3), 1.31 (t, 3H, $J_{H,H}$= 7.1 Hz, CH_2-CH_3) ppm; ^{13}C-NMR (75.5 MHz, $CDCl_3$) δ 169.5 (C=O), 166.1 (C=O), 152.7 (=CH-N), 145.5, 130.7, 119.2, 114.3 (Ar-C), 91.9 (*C*=CH), 60.3 (CH_2O), 60.0 (CH_2O), 44.7, 33.9, 32.7, 29.2, 28.0, 26.4 (CH_2), 14.6, 14.5 (2CH_3) ppm; HRESI-MS calcd. for $C_{20}H_{30}{}^{79}BrN_2O_4$ **(**$[M+H]^+$): 441.1383, found: 441.1382; calcd. for $C_{20}H_{30}{}^{81}BrN_2O_4$ ($[M+H]^+$): 443.1363, found: 443.1359.

*Diethyl 2-{[(4'-((6''-Thiocyanatohexyl)amino)phenyl)amino]methylene}malonate (**22**).* A solution of bromo-derivative **21** (128.4 mg, 0.29 mmol) and KSCN (88.0 mg, 0.91 mmol, 3.1 equiv.) in DMF (2 mL) was heated at 70 ºC in the darkness under Ar for 21 h. After that, it was concentrated to dryness and the residue was purified by column chromatography (cyclohexane → 1:1 Et_2O–cyclohexane) to give **22** as a strongly yellow solid. Yield: 100.6 mg (83%). Mp: 71–79 ºC; ^{1}H-NMR (300 MHz, $CDCl_3$) δ 10.95 (d, 1H, $J_{H,H}$ = 14.1 Hz, Ar-N*H*-C=), 8.40 (d, 1H, $J_{H,H}$ = 14.1 Hz, CH=), 6.99 (m, 2H, Ar-H), 6.63 (m, 2H, Ar-H), 4.28 (q, 2H, $J_{H,H}$ = 7.2 Hz, CH_2-CH_3), 4.22 (q, 2H, $J_{H,H}$ = 7.3 Hz, CH_2-CH_3), 3.11 (t, 2H, $J_{H,H}$ = 7.0 Hz, CH_2-SCN), 2.94 (t, 2H, $J_{H,H}$ = 7.1 Hz, CH_2-N), 1.85 (quint, 2H, $J_{H,H}$ = 7.2 Hz, CH_2), 1.65 (quint, 2H, $J_{H,H}$ = 6.9 Hz, CH_2), 1.48 (m, 4H, 2CH_2), 1.37 (t, 3H, $J_{H,H}$ = 7.0 Hz, CH_2-CH_3), 1.31 (t, 3H, $J_{H,H}$ = 7.1 Hz, CH_2-CH_3) ppm; ^{13}C-NMR (75.5 MHz, $CDCl_3$) δ 169.5 (C=O), 166.1 (C=O), 152.7 (=CH-N), 145.6, 130.6, 119.2, 114.1 (Ar-C), 112.4 (SCN), 91.8 (*C*=CH), 60.3 (*C*H_2-CH_3), 60.0 (*C*H_2-CH_3), 44.5, 34.0, 29.9, 29.2, 27.8, 26.5 (CH_2), 14.6, 14.5 (2CH_3) ppm; HRESI-MS calcd. for $C_{21}H_{30}N_3O_4S$ ($[M+H]^+$): 420.1952, found: 420.1944.

*N-(6'-Thiocyanatohexyl)benzene-1,4-diamine (**23**).* A solution of enamine **22** (231.8 g, 0.55 mmol) and ethylenediamine (270 µL, 4.0 mmol, 7.3 equiv.) in a 2:1 CH_2Cl_2–EtOH mixture was heated at 45 ºC in the darkness under Ar for 6 h. Then, it was concentrated to dryness, and the residue was purified by column chromatography (cyclohexane → 2:1 Et_2O–cyclohexane) to give **23** as a reddish syrup. Yield: 68.1 mg (50%). ^{1}H-NMR (300 MHz, $CDCl_3$) δ 6.59 (m, 4H, m, Ar-H), 3.24 (s, 3H, NH, NH_2), 3.05 (m, 2H, CH_2),

2.93 (t, 2H, $J_{H,H}$ = 7.2 Hz, CH_2), 1.83 (m, 2H, CH_2), 1.61 (m, 2H, CH_2), 1.45 (m, 4H, $2CH_2$) ppm; ^{13}C-NMR (75.5 MHz, $CDCl_3$) δ 141.3 (Ar-C-N), 137.9 (Ar-C-N), 116.9, 114.7 (Ar-C), 112.4 (SCN), 45.1, 34.9, 29.8, 29.4, 27.8, 26.5 (CH_2) ppm; HRESI-MS calcd. for $C_{13}H_{20}N_3S$ ($[M+H]^+$): 250.1372, found: 250.1368.

N-*Biotinyl*-N'*-(6-thiocyanatohexyl)benzene-1,4-diamine (**24**)*. To a solution of D-biotin (67.6 mg, 0.28 mmol) and Et_3N (87 µL, 0.62 mmol, 2.2 equiv.) in DMF (5 mL) was slowly added isobutyl chloroformate (47 µL, 0.36 mmol, 1.3 equiv.); after the addition, the reaction was kept stirring at rt under Ar for 10 min. Then, this mixture was added to a solution of thiocyanate **23** (68.1 mg, 0.27 mmol) in DMF (1 mL), cooled down at 0 ºC; reaction was kept stirring at that temperature for further 5 min, and then, 2.5 h at rt. After that, the mixture was concentrated to dryness and the residue was purified by column chromatography (CH_2Cl_2 → 20:1 CH_2Cl_2-MeOH) to give **24** as a syrup. Yield: 68.4 mg (53%); $[\alpha]_D^{25}$ = +31 (*c* 1.15, $(CD_3)_2SO$); ^{1}H-NMR (500 MHz, $(CD_3)_2SO$) δ 9.41 (s, 1H, Ar-N*H*-CO), 7.25 (m, 2H, Ar-H), 6.47 (m, 2H, Ar-H), 6.42 (s, 1H, s, NH biotin), 6.34 (s, NH biotin), 5.29 (t, 1H, $J_{H,H}$ = 5.6 Hz, CH_2-N*H*), 4.30 (m, 1H, CH-N), 4.14 (m, 1H, CH-N), 3.11 (m, 1H, CH-S), 2.95 (q, 2H, $J_{H,H}$ = 6.7 Hz, CH_2), 2.82 (dd, 1H, $J_{H,H}$ = 5.2 Hz, $J_{H,H}$ = 12.5 Hz, H-C*H*-S), 2.58, (d, 1H, $J_{H,H}$ = 12.3 Hz, H-C*H*-S), 2.22 (t, 2H, $J_{H,H}$ = 7.3 Hz, CH_2-CO), 1.54 (m, 14H, $7CH_2$) ppm; ^{13}C-NMR (125.7 MHz, $(CD_3)_2SO$) δ 170.1 (C=O), 162.7 (C=O), 145.3, 128.3, 120.9 (Ar-C), 113.2 (SCN), 111.7 (Ar-C), 61.0 (NH-CH), 59.2 (NH-CH), 55.4 (S-CH), 43.1, 36.0, 33.2, 29.5, 28.5, 28.3, 28.1, 27.1, 26.0, 25.3 (CH_2) ppm; HRESI-MS calcd. for $C_{23}H_{34}N_5O_2S_2$ ($[M+H]^+$): 476.2148, found: 476.2148.

*6,6'-Dithiobis[*N-*(4''-biotinylamino)phenyl]aminohexyl (**25**)*. To a solution of thiocyanate **24** (58.1 mg, 0.12 mmol) in DMF (1.5 mL) was added $NaBH_4$ (10.0 mg, 0.26 mmol, 2.2 equiv.); reaction was kept stirring at rt for 20 h. Then, it was concentrated to dryness and the residue was purified by column chromatography (CH_2Cl_2 → 5:1 CH_2Cl_2-MeOH) to give **25** as a syrup. Yield: 34.4 mg (64%). $[\alpha]_D^{25}$ = +29 (*c* 0.64, DMSO); ^{1}H-NMR (300 MHz, $(CD_3)_2SO$) δ 9.47 (s, 2H, NH), 7.25 (m, 4H, Ar-H), 6.46 (m, 4H, Ar-H), 6.44 (s, 2H, NH biotin), 6.36 (s, 2H, NH biotin), 5.28 (t, 2H, $J_{H,H}$ = 5.2 Hz, N*H*-CH_2), 4.30 (m, 2H, C*H*-NH), 4.13 (m, 2H, C*H*-NH), 3.11 (m, 2H, CH-S), 2.92 (q, 4H, $J_{H,H}$ = 5.9 Hz, $2CH_2$), 2.82 (dd, 2H, $J_{H,H}$ = 5.1 Hz, $J_{H,H}$ = 12.5 Hz,

H-C*H*-S), 2.69 (t, 4H, $J_{H,H}$ = 7.2 Hz, CH_2-S), 2.57 (d, 2H, $J_{H,H}$ = 12.3 Hz, H-C*H*-S), 2.22 (t, 4H, *J* = 7.2 Hz, 2CH_2-CO), 1.48 (m, 28H 14CH_2) ppm; ^{13}C-NMR (75.5 MHz, $(CD_3)_2SO$) δ 170.1 (C=O), 162.7 (C=O), 145.3, 128.3, 120.9, 111.7 (Ar-C), 61.1(NH-CH), 59.2 (NH-CH), 55.4 (S-CH), 43.1, 37.8, 36.0, 28.6, 28.6, 28.3, 28.1, 27.6, 26.3, 25.3 (CH_2) ppm; HRESI-MS calcd. for $C_{44}H_{67}N_8NaO_4S_4$ ($[M+H]^+$): 899.4163, found: 899.4144.

N-*[4-(Biotinylamino)phenyl]formamide (**26**)*. A solution of amino derivative **4** (120.0 mg, 0.36 mmol) and AcOH (21 µL, 0.36 mmol, 1.0 equiv.) in ethyl formate (5 mL) was refluxed for 3.5 h. The resulting precipitate was filtered, washed with ethyl formate (5 mL) and centrifuged at 3,000 rpm for 2 min twice to give **26** as a white solid. Yield: 118.1 mg (98%). Mp: 188-196 ºC; $[\alpha]_D^{24}$ = +41 (*c* 0.81, DMSO); ^{1}H-NMR (300 MHz, $(CD_3)_2SO$) δ 9.45 (s, 1H, CHO), 7.21 (m, 2H, Ar-H), 6.50 (m, 2H, Ar-H), 6.44 (s, 1H, NH), 6.36 (s, 1H, NH), 5.04 (s, 2H, 2NH), 4.30 (m, 1H, C*H*-NH), 4.13 (m, 1H, C*H*-NH), 3.11 (m, 1H, CH-S), 2.82 (dd, 1H, $J_{H,H}$ = 5.2 Hz, $J_{H,H}$ = 12.5 Hz, H-C*H*-S), 2.57 (d, 1H, $J_{H,H}$ = 12.2 Hz, H-C*H*-S), 2.22 (t, 2H, $J_{H,H}$ = 7.3 Hz, CH_2), 1.48 (m, 6H, 3CH_2) ppm; ^{13}C-NMR (75.5 MHz, $(CD_3)_2SO$) δ 170.1 (C=O), 162.7 (C=O), 144.0, 128.9, 120.8, 114.0 (Ar-C), 61.0 (NH-CH), 59.2 (NH-CH), 55.4 (S-CH), 39.8 (S-CH_2), 36.0, 28.2, 28.1, 25.3 (CH_2) ppm; HRESI-MS calcd. for $C_{17}H_{23}N_4O_3S$ ($[M+H]^+$): 363.1485, found: 363.1500.

N-*[4-(Biotinylamino)phenyl]*-N'-*(4-iodophenyl)selenourea (**27**)*. To a solution of amino derivative **4** (46.0 mg, 0.14 mmol) in DMF (2 mL) was added 4-iodophenyl isoselenocyanate (50.3 mg, 0.16 mmol, 1.1 equiv.). The resulting mixture was heated at 45 ºC in the darkness under Ar for 2 h. Then, it was concentrated to dryness, and the residue was washed with EtOH (15 mL) and centrifuged at 3,000 rpm during 2 min twice, to give **27** as a grey solid. Yield: 51.6 mg (57%). Mp: 187–195 ºC; $[\alpha]_D^{23}$ = +24 (*c* 0.80, DMSO); ^{1}H-NMR (300 MHz, $(CD_3)_2SO$) δ 10.16 (s, 1H, NH), 10.00 (s, 1H, NH), 9.91 (s, 1H, NH), 7.65 (m, 2H, Ar-H), 7.55 (m, 2H, Ar-H), 7.24 (m, 4H, Ar-H), 6.43 (s, 1H, biotin), 6.36 (s, 1H, NH biotin), 4.30 (m, 1H, CH-N), 4.14 (m, 1H, CH-N), 3.12 (m, 1H, CH-S), 2.82 (dd, 1H, $J_{H,H}$ = 12.4 Hz, $J_{H,H}$ = 5.0 Hz, H-C*H*-S), 2.57 (d, 1H, $J_{H,H}$ = 12.6 Hz, H-C*H*-S), 2.30 (t, 2H, $J_{H,H}$ = 7.3 Hz, CH_2-CO), 1.51 (m, 6H, 3CH_2) ppm; ^{13}C-

NMR (75.5 MHz, $(CD_3)_2SO$) δ 179.0 (C=Se), 171.6 (C=O), 163.2 (C=O), 140.2, 137.6, 137.4, 134.7, 127.5, 125.9, 119.7 (Ar-C), 90.2 (Ar-C-I), 61.5 (CH-NH), 59.7 (CH-NH), 55.9 (CH-S), 36.7, 28.7, 28.6, 25.6 (CH_2) ppm; HRESI-MS calcd. for $C_{23}H_{26}IN_5NaO_2SSe$ ($[M+Na]^+$): 665.9909, found: 665.9892.

tert-*Butyl {4-[(6'-selenocyanatohexyl)amino]phenyl}carbamate (**28**).* A solution of bromo-derivative **18** (224.5 mg, 0.60 mmol) and KSeCN (258.8 mg, 1.80 mmol, 3.0 equiv.) in DMF (6 mL) was heated at 70 ºC in the darkness under Ar for 2.5 h. Then it was concentrated to dryness and the residue was purified by column chromatography (cyclohexane → 1:4 EtOAc–cyclohexane) to give **28** as a red syrup. Yield: 124.7 mg (52%). ^{1}H-NMR (300 MHz, $CDCl_3$) δ 6.93 (m, 2H, Ar-H), 6.69 (m, 2H, Ar-H), 3.77 (brs, 2H, 2NH), 3.54 (t, 2H, $J_{H,H}$ = 7.2 Hz, CH_2), 3.01 (t, 2H, $J_{H,H}$ = 7.3 Hz, CH_2), 1.86 (m, 2H, CH_2), 1.42 (m, 6H, $3CH_2$), 1.40 (s, 9H, $C(CH_3)_3$) ppm; ^{13}C-NMR (300 MHz, $CDCl_3$) δ 155.4 (C=O), 144.5, 134.3, 128.4, 116.0 (Ar-C), 101.7 (SeCN), 79.8 ($C(CH_3)_3$), 49.9, 30.9, 29.6, 28.9 (CH_2), 28.5 ($C(CH_3)_3$), 27.7, 26.0 (CH_2) ppm; HRESI-MS calcd. for $C_{18}H_{28}N_3O_2{}^{80}Se$ ($[M+H]^+$): 398.1341, found: 398.1335.

*Diethyl 2-{[(4'-((6''-selenocyanatohexyl)amino)phenyl)amino]methylene}malonate (**29**).* A solution of bromo-derivative **21** (100.6 mg, 0.23 mmol) and KSeCN (97.8 mg, 0.68 mmol, 3.0 equiv.) in DMF (2 mL) was heated at 70 ºC in the darkness under Ar for 3.5 h. Then, it was concentrated to dryness and the residue was purified by column chromatography (cyclohexane → 1:2 EtOAc–cyclohexane) to give **29** as a syrup. Yield: 95.4 mg (90%); ^{1}H-NMR (300MHz, $(CD_3)_2CO$) δ 10.85 (d, 1H, $J_{H,H}$ = 13.9 Hz, Ar-N*H*-C=), 8.38 (d, 1H, $J_{H,H}$ = 14.0 Hz, C*H*=), 7.10 (m, 2H, Ar-H), 6.68 (m, 2H, Ar-H), 5.01 (t, 1H, $J_{H,H}$ = 5.0 Hz, NH), 4.21 (q, 2H, $J_{H,H}$ = 7.1 Hz, C*H*$_2$-CH_3), 4.14 (q, 2H, $J_{H,H}$ = 7.1 Hz, C*H*$_2$-CH_3), 3.19 (t, 2H, $J_{H,H}$ = 7.1 Hz, CH_2), 3.13 (t, 2H, $J_{H,H}$ = 7.1 Hz, CH_2), 1.93 (m, 2H, CH_2), 1.67 (m, 2H, CH_2), 1.52 (m, 4H, $2CH_2$), 1.27 (m, 6H, $2CH_2$-C*H*$_3$) ppm; ^{13}C-NMR (75.5 MHz, $(CD_3)_2CO$) δ 169.6 (C=O), 166.0 (C=O), 153.1 (=CH-N-), 148.1, 130.1, 119.9, 113.8 (Ar-C), 102.7 (SeCN), 92.2 (*C*=CH), 60.2 (*C*H_2-CH_3), 59.9 (*C*H_2-CH_3), 44.3, 31.9, 30.1, 29.5, 27.1 (CH_2), 14.8, 14.7 ($2CH_3$) ppm; HRESI-MS calcd. for $C_{21}H_{30}N_3O_4{}^{80}Se$ ($[M+H]^+$): 468.1396, found: 468.1396.

N-*(6'-Selenocyanatohexyl)benzene-1,4-diamine (**30**)*. To a solution of enamine **29** (241.3 mg, 0.52 mmol) in EtOH (6 mL) was added ethylenediamine (175 µL, 2.62 mmol, 5.0 equiv.), and the corresponding mixture was stirred at rt in the darkness under Ar for 16 h. Then, it was concentrated to dryness and the residue was purified by column chromatography (cyclohexane → 2:1 EtOAc–cyclohexane) to give **30** as a syrup. Yield: 105.5 mg (68%); ^{1}H-NMR (300 MHz, $(CD_3)_2SO$) δ 6.38 (m, 4H, Ar-H), 4.39 (brs, 3H, NH, NH_2), 3.08 (t, 2H, $J_{H,H}$ = 7.2 Hz, CH_2), 2.88 (m, 2H, CH_2), 1.81 (m, 2H, CH_2), 1.45 (m, 6H, $3CH_2$) ppm; ^{13}C-NMR (75.5 MHz, $(CD_3)_2SO$) δ 140.6, 138.6, 115.6, 113.6, (Ar-C), 104.6 (SeCN), 44.1, 30.8, 29.8, 28.3, 26.0 (CH_2) ppm; HRESI-MS calcd. for $C_{13}H_{20}N_3Se$ ($[M+H]^+$): 298.0817, found: 298.0815.

*N-Biotinyl-N'-(6-selenocyanatohexyl)benzene-1,4-diamine (**31**)*. To a solution of D-biotin (73.9 mg, 0.30 mmol) and Et_3N (96 µL, 0.69 mmol, 2.3 equiv.) in DMF (4.5 mL) was slowly added isobutyl chloroformate (57 µL, 0.44 mmol, 1.5 equiv.); after the addition, the reaction was kept stirring at rt under Ar for 10 min. Then, this mixture was added on a solution of selenocyanate **30** (88.8 mg, 0.30 mmol, 1.0 equiv.) in DMF (1 mL), cooled down at 0 ºC; reaction was kept stirring at that temperature for further 5 min, and then, 2 h at rt. After that, the mixture was concentrated to dryness and the residue was purified by column chromatography (cyclohexane → 5:1 CH_2Cl_2-MeOH) to give **31** as a grey solid. Yield: 79.2 mg (51%). Mp: 141–150 ºC; $[\alpha]_D^{25}$ = +30 (*c* 0.92, DMSO); ^{1}H-NMR (300 MHz, $(CD_3)_2SO$) δ 9.43 (s, 1H, NH), 7.25 (m, 2H, Ar-H), 6.47 (m, 2H, Ar-H), 6.43 (s, 1H, NH biotin), 6.35 (s, 1H, NH biotin), 5.30 (s, 1H, NH), 4.30 (m, 1H, CH-N), 4.14 (m, 1H, CH-N), 3.12 (m, 1H, CH-S), 3.08 (t, 2H, $J_{H,H}$ = 7.3 Hz, CH_2), 2.95 (m, 2H, CH_2), 2.82 (dd, 1H, $J_{H,H}$ = 5.1 Hz, $J_{H,H}$ = 12.4 Hz, H-CH-S), 2.57 (d, 1H, $J_{H,H}$ = 12.5 Hz, H-C*H*-S), 2.22 (t, 2H, $J_{H,H}$ = 7.2 Hz, CH_2-CO), 1.82 (m, 2H, CH_2), 1.49 (m, 12 H, $6CH_2$) ppm; ^{13}C-NMR (75.5 MHz, $(CD_3)_2SO$) δ 170.6 (C=O), 163.2 (C=O), 145.7, 128.8, 121.4, 112.2 (Ar-C), 105.1 (SeCN), 61.5 (NH-CH), 59.7 (NH-CH), 55.9 (S-CH), 43.6, 36.5, 31.2, 30.3, 29.1, 28.7, 28.6, 26.4, 25.8 (CH_2) ppm; HRESI-MS calcd. for $C_{23}H_{34}N_5O_2S^{80}Se$ ($[M+H]^+$): 524.1593, found: 524.1583.

Declaration of competing interest

The authors declare that they have no known competing financial interests or personal relationships that could have appeared to influence the work reported in this paper.

Acknowledgements

We thank Grant PID2020-116460RB-I00 funded by MCIN/AEI/10.13039/501100011033, and Junta de Andalucía (FQM134) for financial support. J.R.-P. thanks the Ministerio de Educación y Ciencia for the award of a predoctoral grant. A.P. and J.M.P. thank the Spanish Government (Project PID2021-123059OB-I00 funded by MCIN/AEI /10.13039/501100011033 / FEDER, UE) for financial support. A.P. thanks the EU Social Fund (FSE) and the Canary Islands ACIISI for a predoctoral grant TESIS2020010055. J.D., S.J.S. and M.P thank the Ministry of Education, Science and Technological Development of the Republic of Serbia for financial support (451-03-68/2022-14/200007). A.P.[d,e] acknowledges the Thailand Development and Promotion of Science and Technology (DPST) Talents Project for funding. This work was performed within the framework of COST Action CA17104 STRATAGEM "New diagnostic and therapeutic tools against multidrug resistant tumors". We would also like to thank the Servicio de Resonancia Magnética Nuclear, CITIUS (University of Seville) for the performance of NMR experiments.

Appendix A. Supplementary data: Table S1 (complete antiproliferative activities), Video S1: Live-cell imaging of untreated SW1573 cells, Video S2: Live-cell imaging of SW1573 cells exposed to compound **31** (100 nM). ^{1}H- and ^{13}C-NMR spectra of new compounds.

References

[1] (last accessed 23rd October 2022), https://www.cancer.gov/about-cancer/understanding/what-is-cancer.

[2] L. Lin, Z. Li, L. Yan, Y. Liu, H. Yang, H. Li, Global, regional, and national cancer incidence and death for 29 cancer groups in 2019 and trends analysis of the global cancer burden, 1990–2019. J. Hematol. Oncol. 14 (2021) 197.

[3] H. Sung, J. Ferlay, R.L. Siegel, M. Laversanne, I. Soerjomataram, A. Jemal, F. Bray, Global cancer statistics 2020: GLOBOCAN estimates of incidence and mortality worldwide for 36 cancers in 185 countries. CA Cancer J. Clin. 71 (2021) 209–249.

[4] R.L. Siegel, K.D. Miller, H.E. Fuchs, A. Jemal, Cancer Statistics, 2021. CA Cancer J. Clin. 71 (2021) 7–33.

[5] (last accessed 23rd October 2022), https://www.who.int/news-room/fact-sheets/detail/cancer.

[6] A. Franconetti, Ó. López, J.G. Fernández-Bolaños, Carbohydrates: potential *sweet* tools against cancer. Curr. Med. Chem. 27 (2020) 1206–1242.

[7] W.M.C. van den Boogaard, D.S.J. Komninos, W.P. Vermeij, Chemotherapy side-effects: not all DNA damage is equal. Cancers 14 (2022) 627.

[8] A. Valente, A. Podolski-Renić, I. Poetsch, N. Filipović, Ó. López, I. Turel, P. Heffeter. Metal- and metalloid-based compounds to target and reverse cancer multidrug resistance. Drug Resist. Updat. 58 (2021) 100778.

[9] P.M. Carrera, H.M. Kantarjian, V.S. Blinder, The Financial burden and distress of patients with cancer: understanding and stepping-up action on the financial toxicity of cancer treatment. CA Cancer J Clin. 68 (2018) 153–165.

[10] L. Falzone, S. Salomone, M. Libra, Evolution of cancer pharmacological treatments at the turn of the third millennium. Front. Pharmacol. 9 (2018) 1300.

[11] C.L. Lorentzen, J.B. Haanen, Ö. Met, I.M. Svane, Clinical advances and ongoing trials of mRNA vaccines for cancer treatment. Lancet Oncol. 23 (2022) e450–e458.

[12] A. Dimitri, F. Herbst, J.A. Fraietta, Engineering the next-generation of CAR T-cells with CRISPR-Cas9 gene editing. Mol. Cancer 21 (2022) 78.

[13] A. Archilla-Ortega, C. Domuro, J. Martin-Liberal, P. Muñoz, Blockade of novel immune checkpoints and new therapeutic combinations to boost antitumor immunity. J. Exp. Clin. Cancer Res. 41 (2022) 62.

[14] T. Olivier, A. Haslam, V. Prasad, Anticancer drugs approved by the US Food and Drug Administration from 2009 to 2020 according to their mechanism of action. JAMA Netw. Open 4 (2021) e2138793.

[15] C.W. Nogueira, N.V. Barbosa, J.B.T. Rocha, Toxicology and pharmacology of synthetic organoselenium compounds: an update. Arch. Toxicol. 95 (2021) 1179–1226.

[16] H. Chuai, S.-Q. Zhang, H. Bai, J. Li, Y. Wang, J. Sun, E. Wen, J. Zhang, M. Xin, Small molecule selenium-containing compounds: Recent development and therapeutic applications. Eur. J. Med. Chem. 223 (2021) 113621.

[17] A.C. Ruberte, C. Sanmartin, C. Aydillo, A.K. Sharma, D. Plano, Development and therapeutic potential of selenazo compounds. J. Med. Chem. 63 (2020) 1473–1489.

[18] L. Kuršvietiene, A. Mongirdiene, J. Bernatoniene, J. Šulinskiene, I. Stanevičiene, Selenium anticancer properties and impact on cellular redox status. Antioxidants 9 (2020) 80.

[19] Z. Qiao, N. Wei, L. Jin, H. Zhang, J. Luo, Y. Zhang K. Wang, The Mpro structure-based modifications of ebselen derivatives for improved antiviral activity against SARS-CoV-2 virus. Bioorg. Chem. 117 (2021) 105455.

[20] C.S. García, E.M. Besckow, C.N. da Silva Espíndola, G. D'Avila Nunes, N.P. Zuge, M.P. de Azeredo, M.J. da Rocha, L.R. Carraro Jr., F. Penteado, C.S. Gomes, E.J. Lenardão, C.F. Bortolatto, C.A. Brüning, Antidepressant-like effect of a selenoindolizine in mice: *in vivo* and *in silico* evidence for the involvement of the serotonergic 5-HT2A/C receptors. ACS Chem. Neurosci. 13(2022) 1746–1755.

[21] V. Burmistrov, C. Morisseau, D.A. Babkov, T. Golubeva, D. Pitushkin, E.V. Sokolova, V. Vasipov, Y. Kuznetsov, S.V. Bazhenov, U.S. Novoyatlova, N.A. Bondarev, I.V. Manukhov, V. Osipova, N. Berberova, A.A. Spasov, G.M. Butov, B.D. Hammock, Anti-inflammatory activity of soluble epoxide hydrolase inhibitors based on selenoureas bearing an adamantane moiety. Int. J. Mol. Sci. 23 (2022) 10710.

[22] K.N.B. Ledebuhr, G. D'Avila Nunes, E.M. Besckow, M.R. Giehl, B. Godoi, C.F. Bortolatto, C.A. Brüning, Antinociceptive effect of *N*-(3-(phenylselanyl)prop-2-yn-1-yl)benzamide in mice: Involvement of 5-HT_{1A} and 5-$HT_{2A/2C}$ receptors. Chem. Biol. Interact. 359 (2022) 109918.

[23] A. Ibáñez-Escribano, C. Fonseca-Berzal, M. Martínez-Montiel, M. Álvarez-Márquez, M. Gómez-Núñez, M. Lacueva-Arnedo, T. Espinosa-Buitrago, T. Martín-Pérez, J.A. Escario, P. Merino-Montiel, S. Montiel-Smith, A. Gómez-Barrio, Ó. López, J.G. Fernández-Bolaños, Thio- and selenosemicarbazones as antiprotozoal agents against *Trypanosoma cruzi* and *Trichomonas vaginalis*. J. Enzyme Inhib. Med. Chem. 37 (2022) 781–791.

[24] V. Alcolea, S. Pérez-Silanes, Selenium as an interesting option for the treatment of Chagas disease: A review. Eur. J. Med. Chem. 206 (2020) 112673.

[25] G. Provensi, A. Costa, B. Rani, M.V. Becagli, F. Vaiano, M.B. Passani, D. Tanini, A. Capperucci, S. Carradori, J.P. Petzer, A. Petzer, D. Vullo, G. Costantino, P. Blandina, A. Angeli, C.T. Supuran, New β-arylchalcogeno amines with procognitive properties targeting carbonic anhydrases and monoamine oxidases. Eur J. Med. Chem. 244 (2022) 114828.

[26] A. Angeli, D. Tanini, A. Nocentini, A. Capperucci, M. Ferraroni, P. Gratteri, C.T. Supuran, Selenols: a new class of carbonic anhydrase inhibitors. Chem. Commun. 55 (2019) 648–651.

[27] M. Velueta-Viveros, M. Martínez-Bailén, A. Puerta, L.L. Romero-Hernández, V. Křen, P. Merino-Montiel, S. Montiel-Smith, M.X. Fernandes, A.J. Moreno-Vargas, J.M. Padrón, Ó. López, J.G. Fernández-Bolaños, Carbohydrate-derived bicyclic selenazolines as new dual

inhibitors (cholinesterases/OGA) against Alzheimer's disease. Bioorg. Chem. 127 (2022) 105983.

[28] J.M. Roldán-Peña, D. Alejandre-Ramos, Ó. López, I. Maya, I. Lagunes, J.M. Padrón, L.E. Peña-Altamira, M. Bartolini, B. Monti, M.L. Bolognesi, J.G. Fernández-Bolaños, New tacrine dimers with antioxidant linkers as dual drugs: Anti-Alzheimer's and antiproliferative agents. Eur. J. Med. Chem. 138 (2017) 761–773.

[29] I. Lagunes, P. Begines, A. Silva, A.R. Galán, A. Puerta, M.X. Fernandes, I. Maya, J.G. Fernández-Bolaños, Ó. López, J.M. Padrón, Selenocoumarins as new multitarget antiproliferative agents: Synthesis, biological evaluation and *in silico* calculations. Eur. J. Med. Chem. 179 (2019) 493–501.

[30] C. Tang, Y. Du, Q. Liang, Z. Cheng, J. Tian, A selenium-containing selective histone deacetylase 6 inhibitor for targeted in vivo breast tumor imaging and therapy. J. Mat. Chem. B, 7 (2019) 3528–3536.

[31] J.I. Olsen, G.B. Plata, J.M. Padrón, Ó. López, M. Bols, J.G. Fernández-Bolaños, Selenoureido-iminosugars: A new family of multitarget drugs. Eur. J. Med. Chem. 123 (2016) 155–160.

[32] F.S. de Oliveira Pereira, F.A.R. Barbosa, R.F.S. Canto, C. Lucchese, S. Pinton, A.L. Braga, J.B. de Azeredo, C.B. Quines, D.S. Ávila, Dihydropyrimidinone-derived selenoesters efficacy and safety in an in vivo model of Aβ aggregation. NeuroToxicology 88 (2022) 14–24.

[33] Z. Chen, H. Lai, L. Houa, T. Chen, Rational design and action mechanisms of chemically innovative organoselenium in cancer therapy. Chem. Commun. 56 (2020) 179–196.

[34] L. Wang, W. Zheng, X. Jiang, Benzeneselenol-modified gold nanoclusters for cancer therapy, Chem. Commun. 56 (2020) 6664–6667.

[35] P. Garnica, I. Encío, D. Plano, J.A. Palop, C. Sanmartín, Organoseleno cytostatic derivatives: Autophagic cell death with AMPK and JNK activation. Eur. J. Med. Chem. 175 (2019) 234–246.

[36] E.E. Frieben, S. Amin, A.K. Sharma, Development of isoselenocyanate compounds' syntheses and biological applications. J. Med. Chem. 62 (2019) 5261–5275.

[37] F.A.R. Barbosa, T. Siminski, R.F.S. Canto, G.M. Almeida, N.S.R.S. Mota, F. Ourique, R.C. Pedrosa, A.L. Braga, Eur. J. Med. Chem. 155 (2018) 503–515.

[38] B. An, B. Wang, J. Hu, S. Xu, L. Huang, X. Li. A.S.C. Chan, Synthesis and biological evaluation of selenium-containing 4-anilinoquinazoline derivatives as novel antimitotic agents. J. Med. Chem. 61 (2018) 2571–2588.

[39] A. Fuentes-Aguilar, L.L. Romero-Hernández, A. Arenas-González, P. Merino-Montiel, S. Montiel-Smith, S. Meza-Reyes, J.L. Vega-Báez, G.B. Plata, J.M. Padrón, Ó. López, J.G.

Fernández-Bolaños, New selenosteroids as antiproliferative agents. Org. Biomol. Chem. 15 (2017) 5041–5054.

[40] V. Calcatierra, Ó. López, J.G. Fernández-Bolaños, G.B. Plata, J.M. Padrón, Phenolic thio- and selenosemicarbazones as multi-target drugs. Eur. J. Med. Chem. 94 (2015) 63–72.

[41] S. Maiti, P. Paira, Biotin conjugated organic molecules and proteins for cancer therapy: A review. Eur. J. Med. Chem. 145 (2018) 206–223.

[42] I. Ojima, X. Wang, Y. Jing, C. Wang, Quest for efficacious next-generation taxoid anticancer agents and their tumor-targeted delivery. J. Nat. Prod. 81 (2018) 703–721.

[43] S. Park, E. Kim, W.Y. Kim, C. Kang, J.S. Kim, Biotin-guided anticancer drug delivery with acidity-triggered drug release. Chem. Commun. 51 (2015) 9343–9345.

[44] S. Maiti, N. Park, J.H. Han, H.M. Jeon, J.H. Lee, S. Bhuniya, C. Kang, J.S. Kim, Gemcitabine–coumarin–biotin conjugates: a target specific theranostic anticancer prodrug. J. Am. Chem. Soc. 135 (2013) 4567–4572.

[45] E. Gil de Montes, A. Istrate, C.D. Navo, E. Jiménez-Moreno, E.A. Hoyt, F. Corzana, I. Robina, G. Jiménez-Osés, A.J. Moreno-Vargas, G.J.L. Bernardes, Stable pyrrole-linked bioconjugates through tetrazine-triggered azanorbornadiene fragmentation. Angew. Chem. Int. Ed. 59 (2020) 6196–6200.

[46] Y.-G. Zheng, X.-Q. Wu, J. Su, P. Jiang, L. Xu, J. Gao, B. Cai, M. Ji, Design and synthesis of a novel photoaffinity probe for labelling EGF receptor tyrosine kinases. J. Enzyme Inhib. Med. Chem. 32 (2017) 954–959.

[47] M. Togashi, Y. Urano, H. Kojima, T. Terai, K. Hanaoka, K. Igarashi, Y. Hirata, T. Nagano, Sensitive detection of acrolein in serum using time-resolved luminescence. Org. Lett. 12 (2010) 1704–1707.

[48] A. Ilangovan, R.G. Kumar, 2,2-Bis(ethoxycarbonyl)vinyl (BECV) as a versatile amine protecting group for selective functional-group transformations. Chem. Eur. J. 16 (2010) 2938–2943.

[49] Ó. López, S. Maza, V. Ulgar, I. Maya, J.G. Fernández-Bolaños, Synthesis of sugar-derived isoselenocyanates, selenoureas, and selenazoles. Tetrahedron 65 (2009) 2556–2566.

[50] H. Elshaflu, T.R. Todorović, M. Nikolić, A. Lolić, A. Višnjevac, S. Hagenow, J.M. Padrón, A.T. García-Sosa, L.S. Djordjević, S. Grubišić, H. Stark, N.R. Filipović, Selenazolyl-hydrazones as novel selective MAO inhibitors with antiproliferative and antioxidant activities: experimental and *in-silico* studies. Front. Chem. 6 (2018) 247.

[51] K. Bukowski, M. Kciuk, R. Kontek, Mechanisms of multidrug resistance in cancer chemotherapy. Int. J. Mol. Sci. 21 (2020) 3233.

[52] T. Alexa-Stratulat, M. Pešić, A.Č. Gašparović, I.P. Trougakos, C. Riganti, What sustains the multidrug resistance phenotype beyond ABC efflux transporters? Looking beyond the tip of the iceberg, Drug Resist. Updat. 46 (2019) 100643.

[53] Y. Tsujimoto, T. Nakagawa, S. Shimizu, Mitochondrial membrane permeability transition and cell death, Biochim. Biophys. Acta 1757 (2006) 1297–1300.

[54] A. Peserico, C. Simone, Physical and functional HAT/HDAC interplay regulates protein acetylation balance. J. Biomed. Biotechnol. 2011, 371832.

[55] K. Pant, E. Peixoto, S. Richard, S.A. Gradilone, Role of histone deacetylases in carcinogenesis: potential role in cholangiocarcinoma. Cells 9 (2020) 780.

[56] G. Li, Y. Tian W.-G, Zhu, The roles of histone deacetylases and their inhibitors in cancer therapy. Front. Cell Dev. Biol. 8 (2020) 576946.

[57] F.J. Hicke, A. Puerta, J. Dinić. M. Pešić, J.M. Padrón, Ó. López, J.G Fernández-Bolaños, Straightforward access to novel mitochondriotropics derived from 2-arylethanol as potent and selective antiproliferative agents. Eur. J. Med. Chem. 228 (2022) 113980.

[58] O. Kepp, L. Galluzzi, M. Lipinski, J. Yuan, G. Kroemer, Cell death assays for drug Discovery. Nat. Rev. Drug Discov. 20 (2011) 221–237.

[59] R. Lacret, A. Puerta, S. Granica, A. González-Bakker, D. Hevia, Y. Teng, C.C. Sánchez-Mateo, P.L. Pérez de Paz, J.M. Padrón, Bioactive potential: a pharmacognostic definition through the screening of four hypericum species from the Canary Islands. Molecules 27 (2022) 6101.

[60] R.E. Barrientos, E. Ibáñez, A. Puerta, J.M. Padrón, A. Paredes, F. Cifuentes, J. Romero-Parra, .J. Palacios, J. Bórquez., M.J. Simirgioti, Phenolic fingerprinting and bioactivity profiling of extracts and isolated compounds from *Gypothamnium pinifolium* Phil. Antioxidants 11 (2022) 2313.

[61] J.M Cross, T.R Blower, A.D.H. Kingdon, R. Pal, D.M. Picton, J.W. Walton, Anticancer Ruthenium complexes with HDAC isoform selectivity. Molecules 25 (2020) 2383.

Figure 1

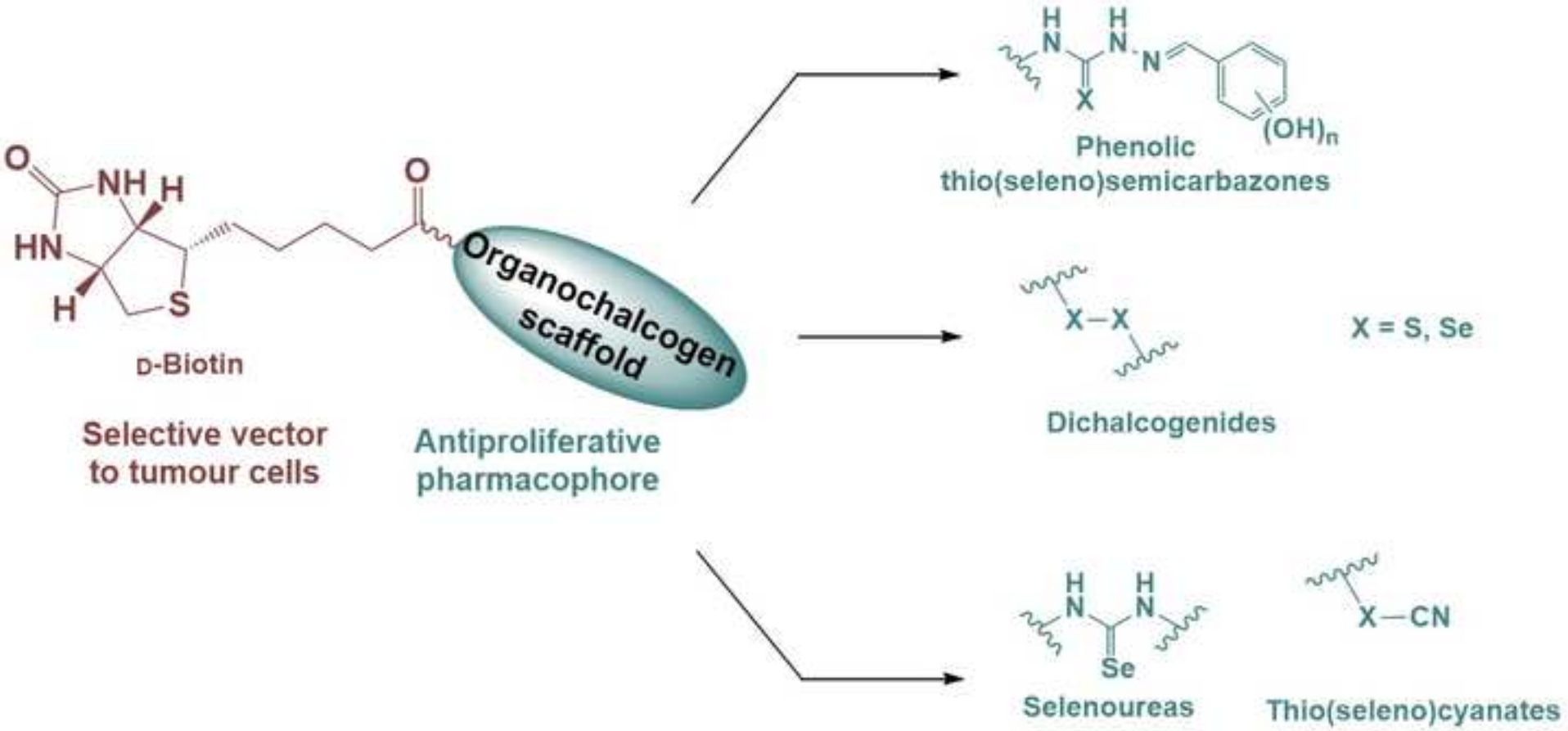

Figure 2

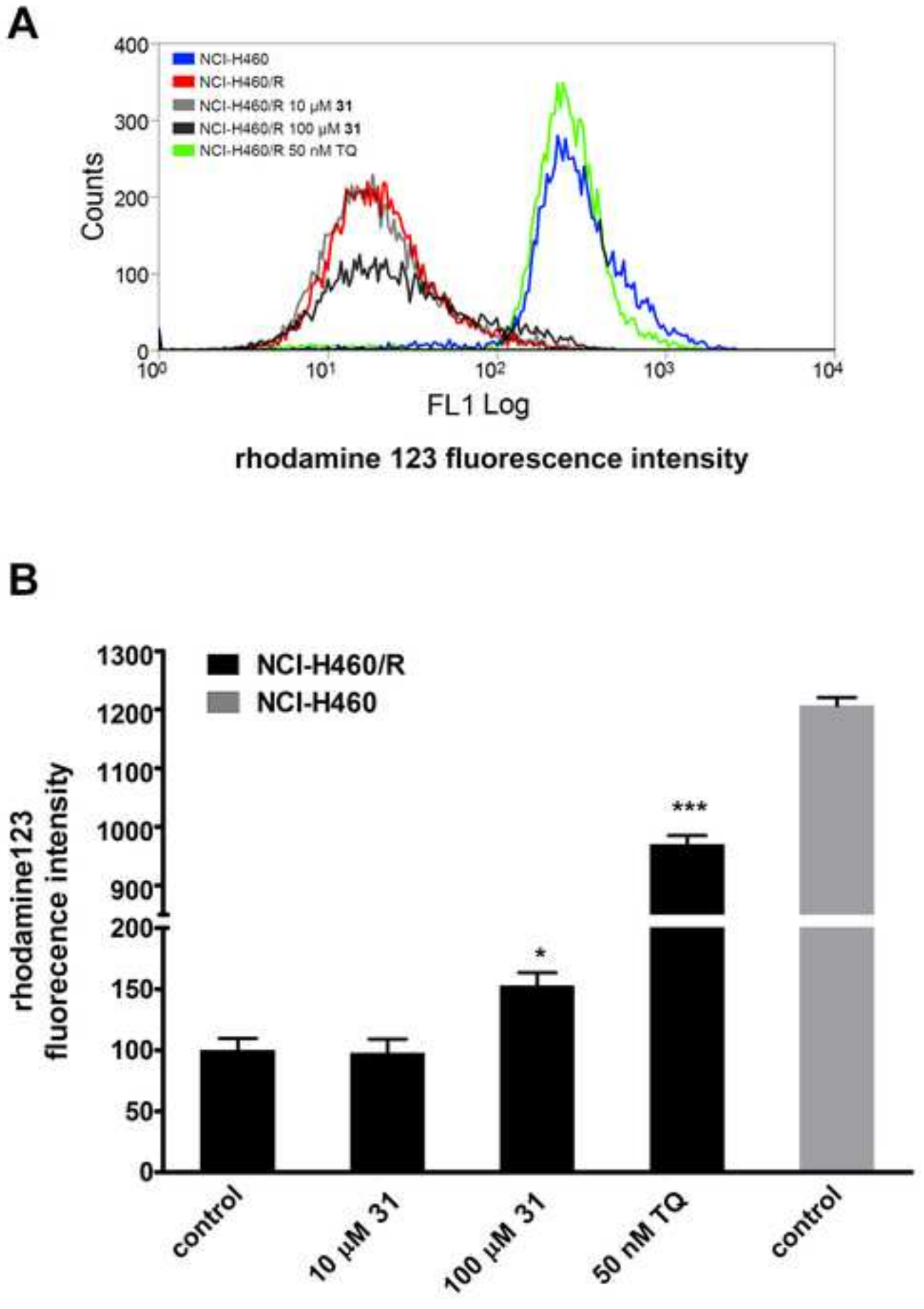

Figure 3

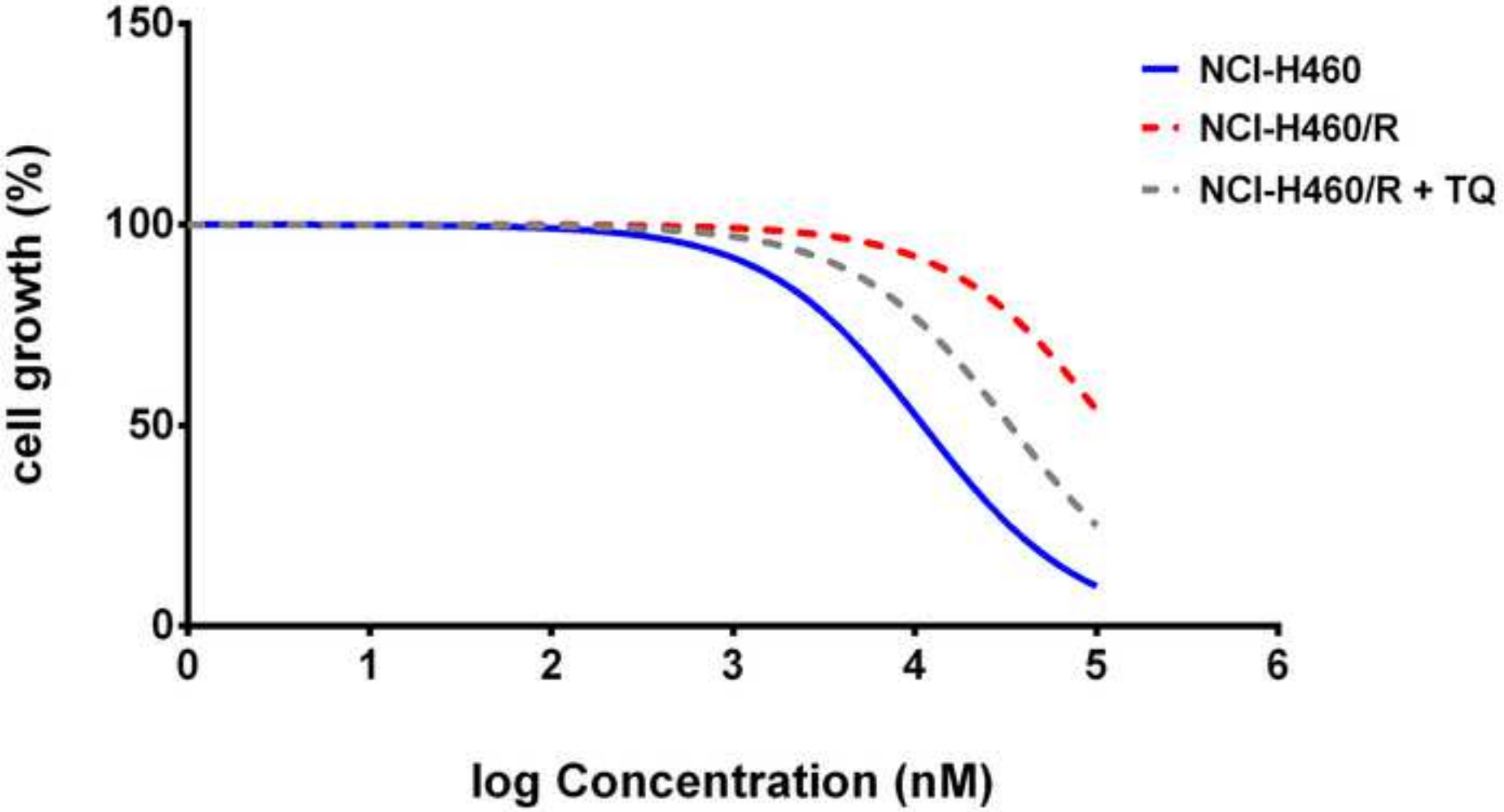

Figure 4

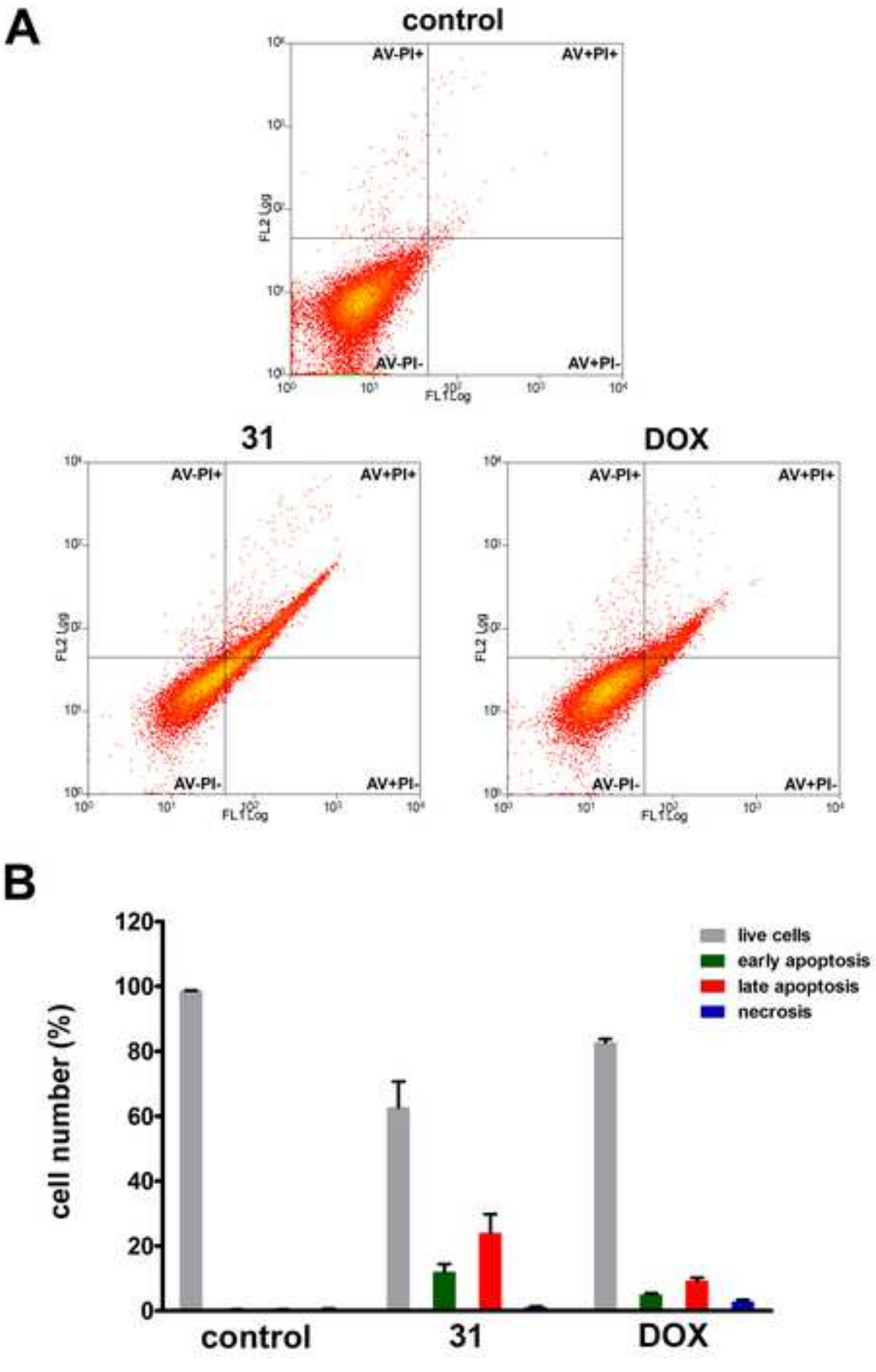

Figure 5

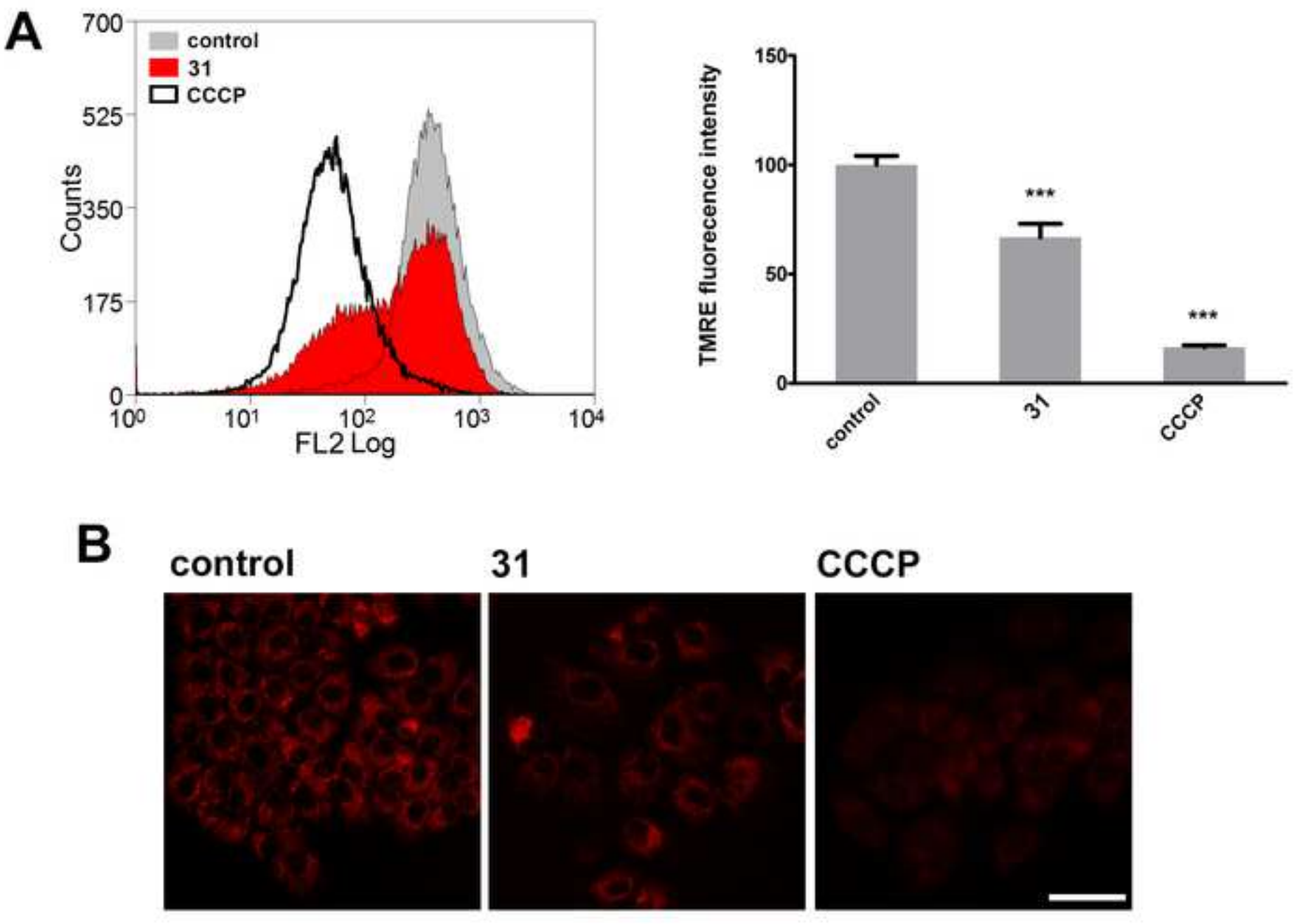

Figure 6

Click here to access/download;Figure;Figure 6.tif

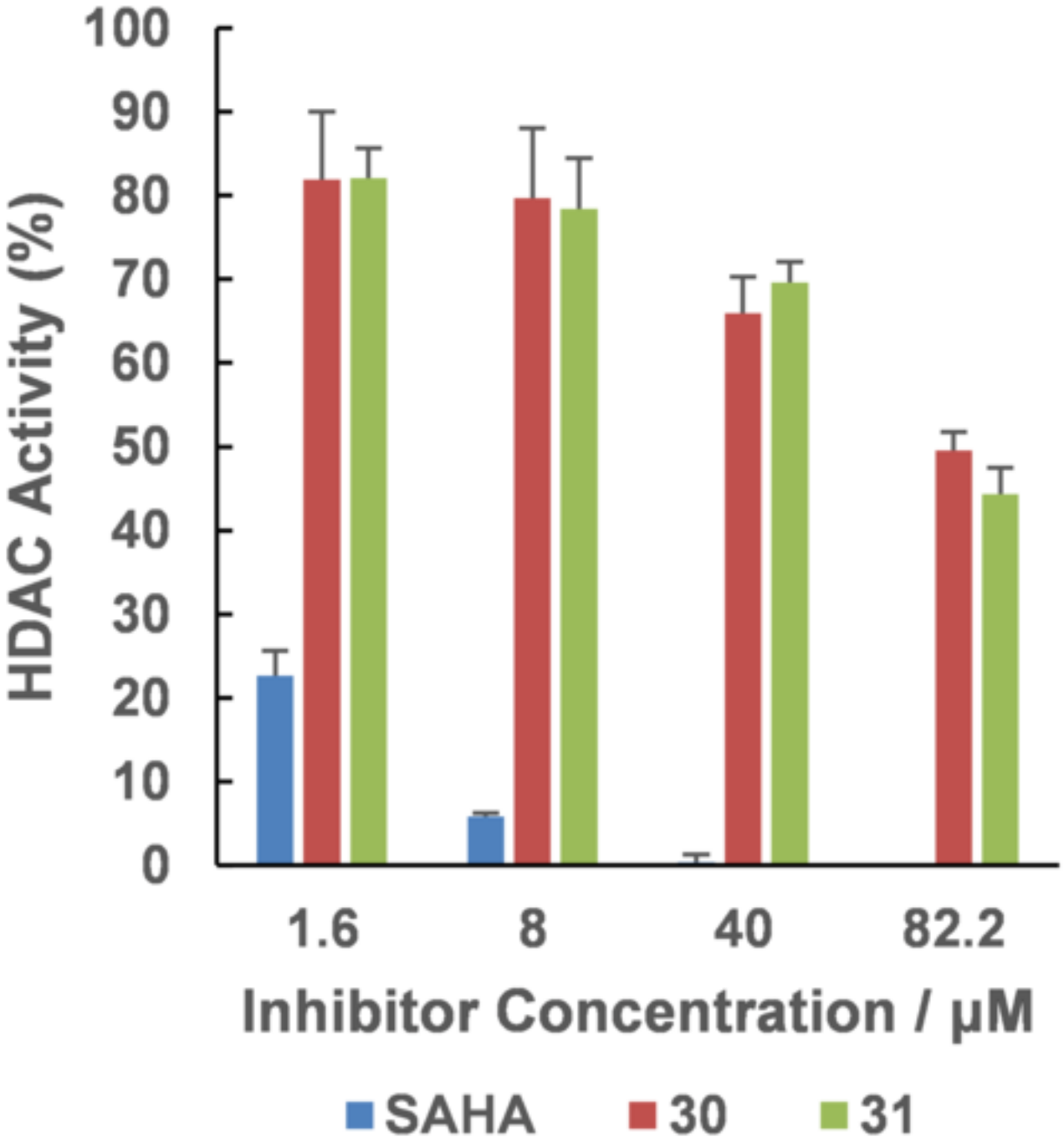

Scheme 1

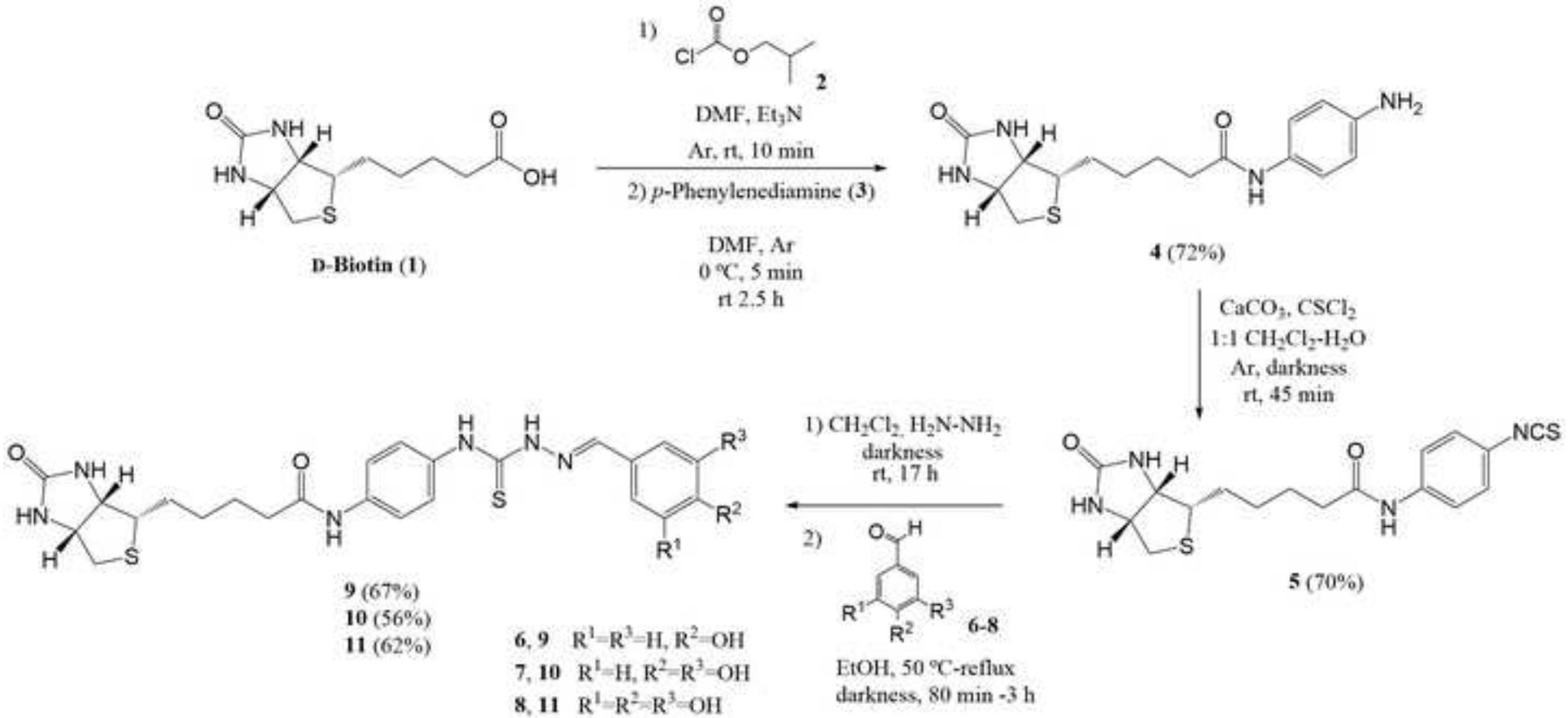

Scheme 2

Click here to access/download;Figure;Scheme 2.jpg

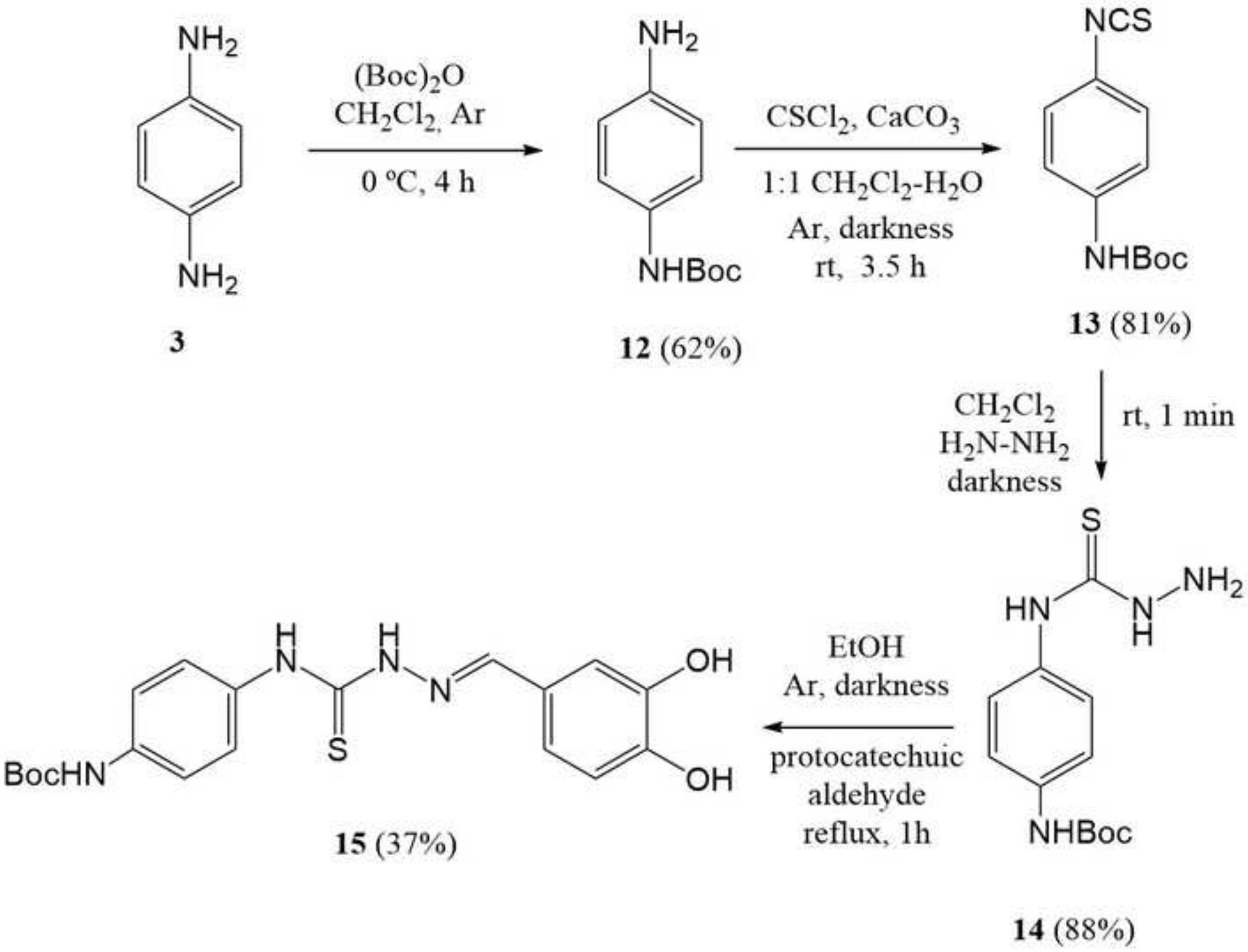

Scheme 3

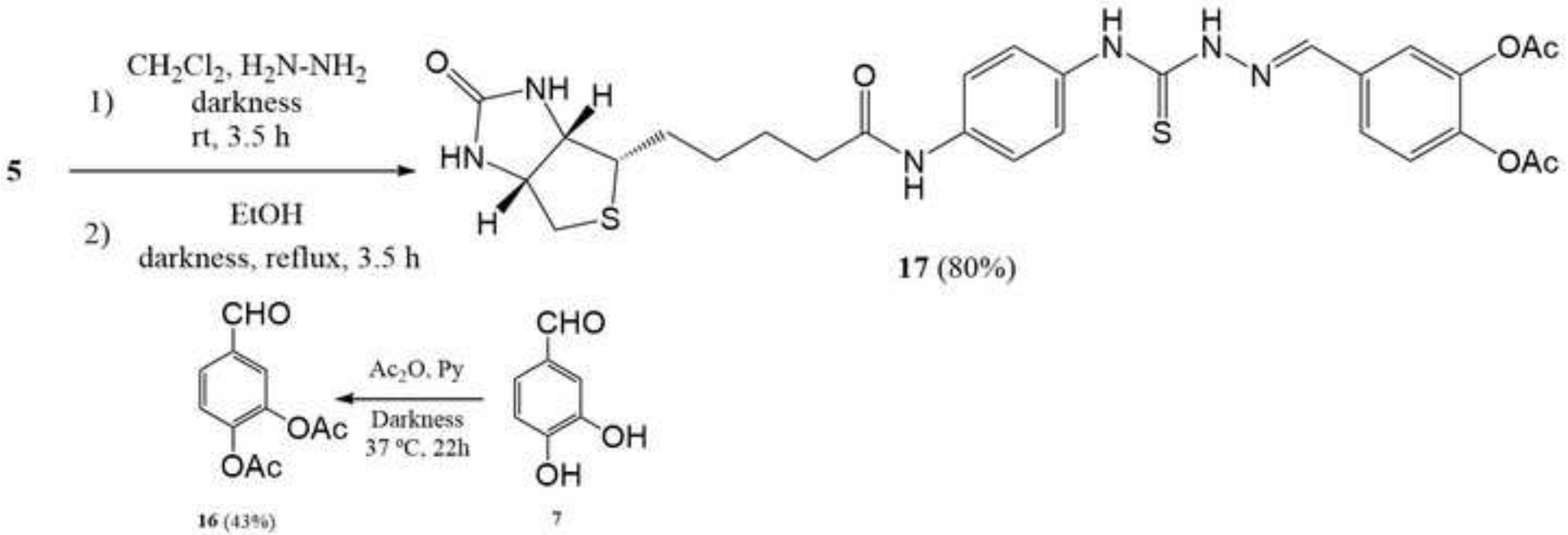

Scheme 4

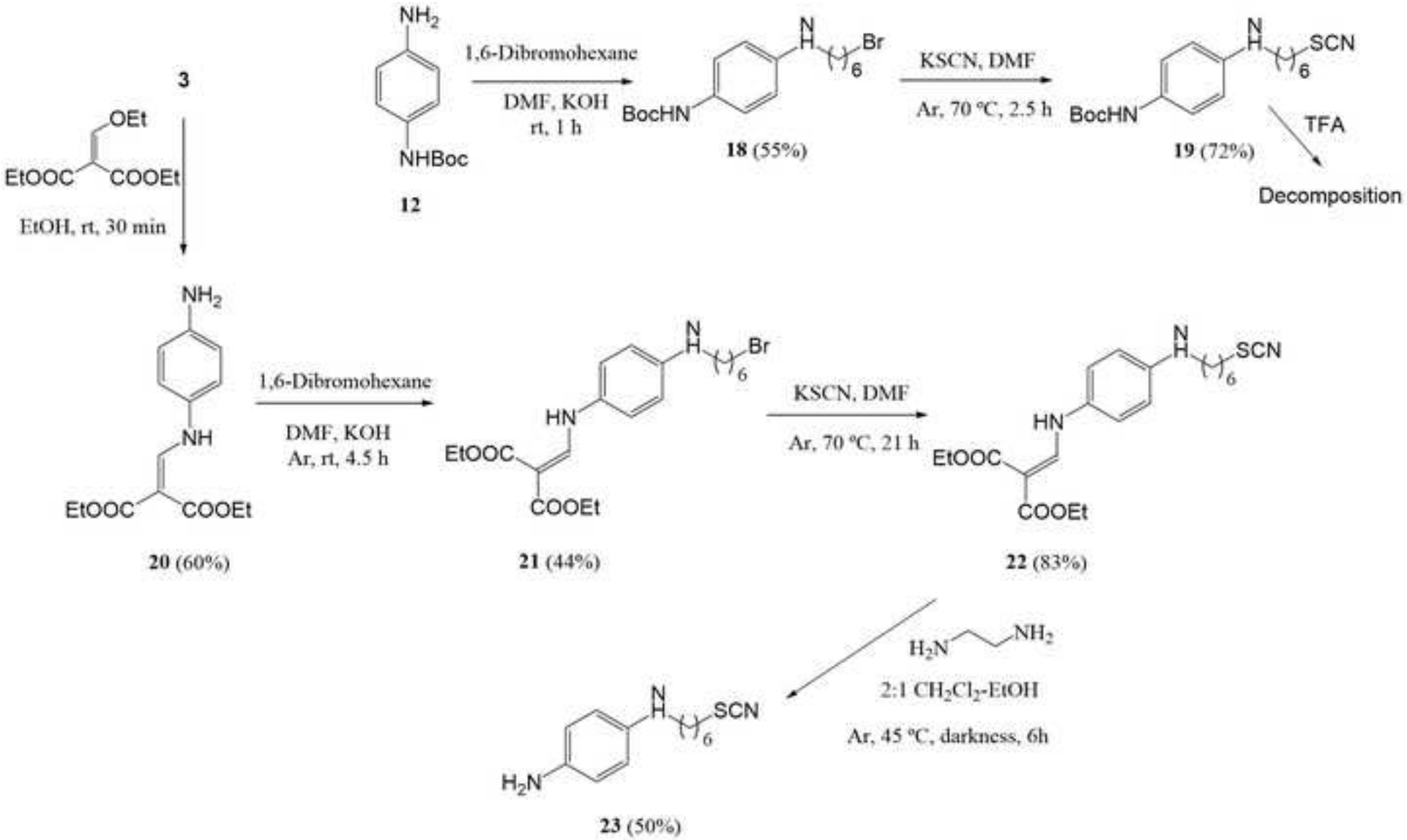

Scheme 5

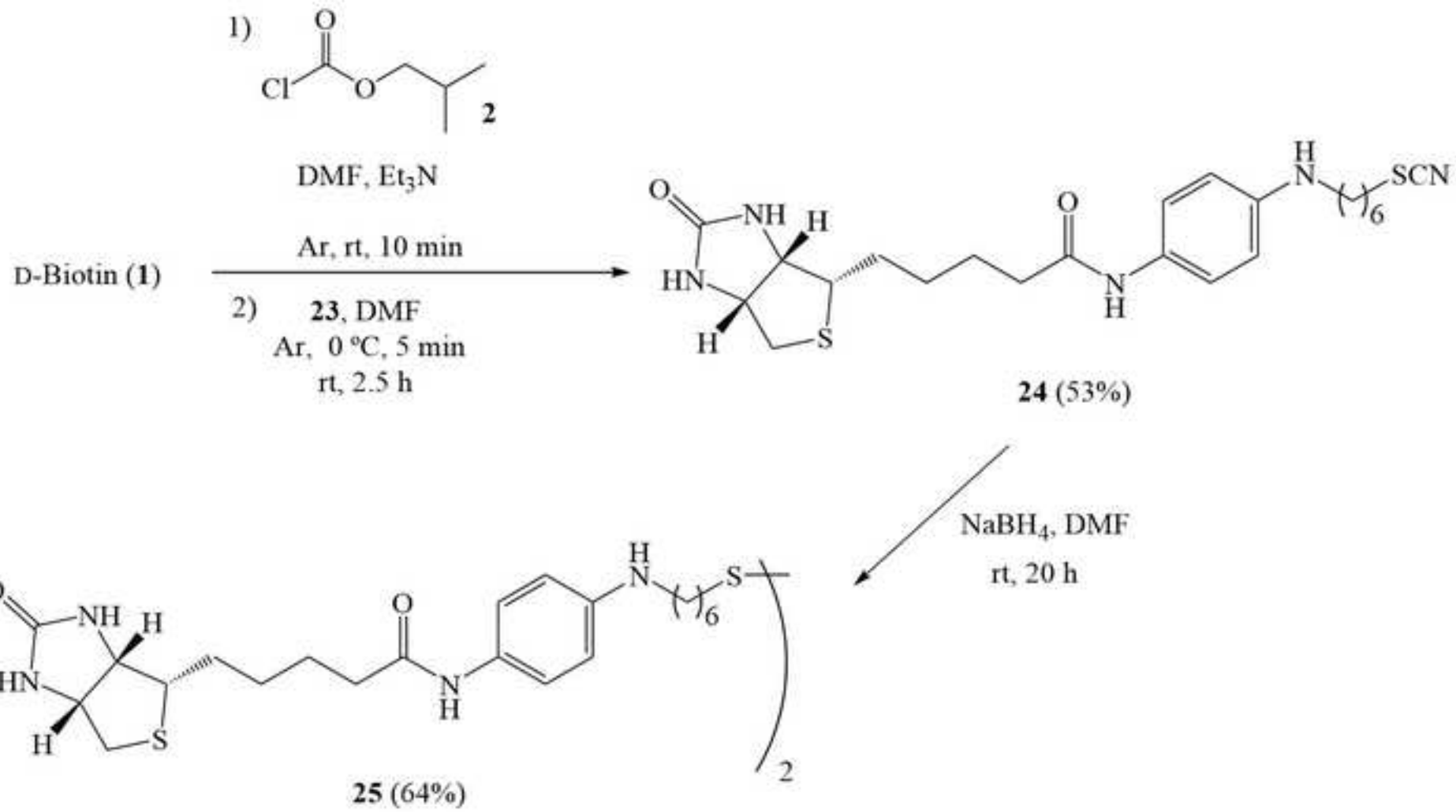

Scheme 6

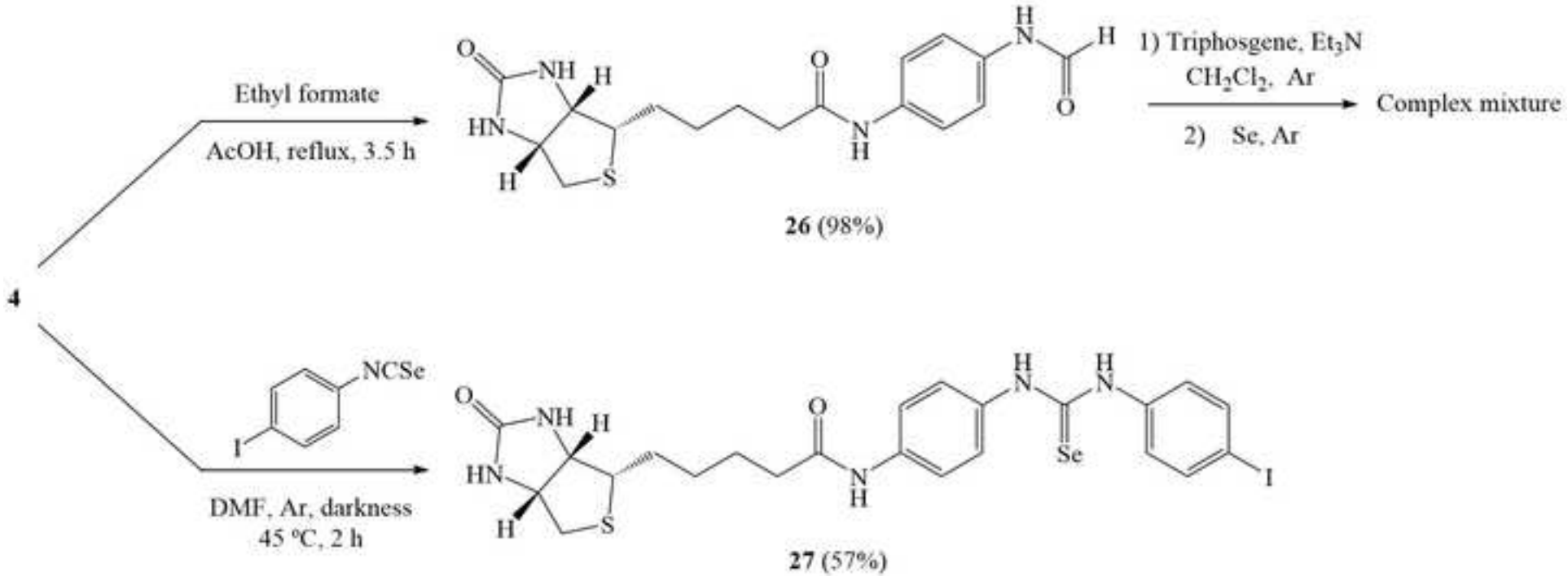

Scheme 7

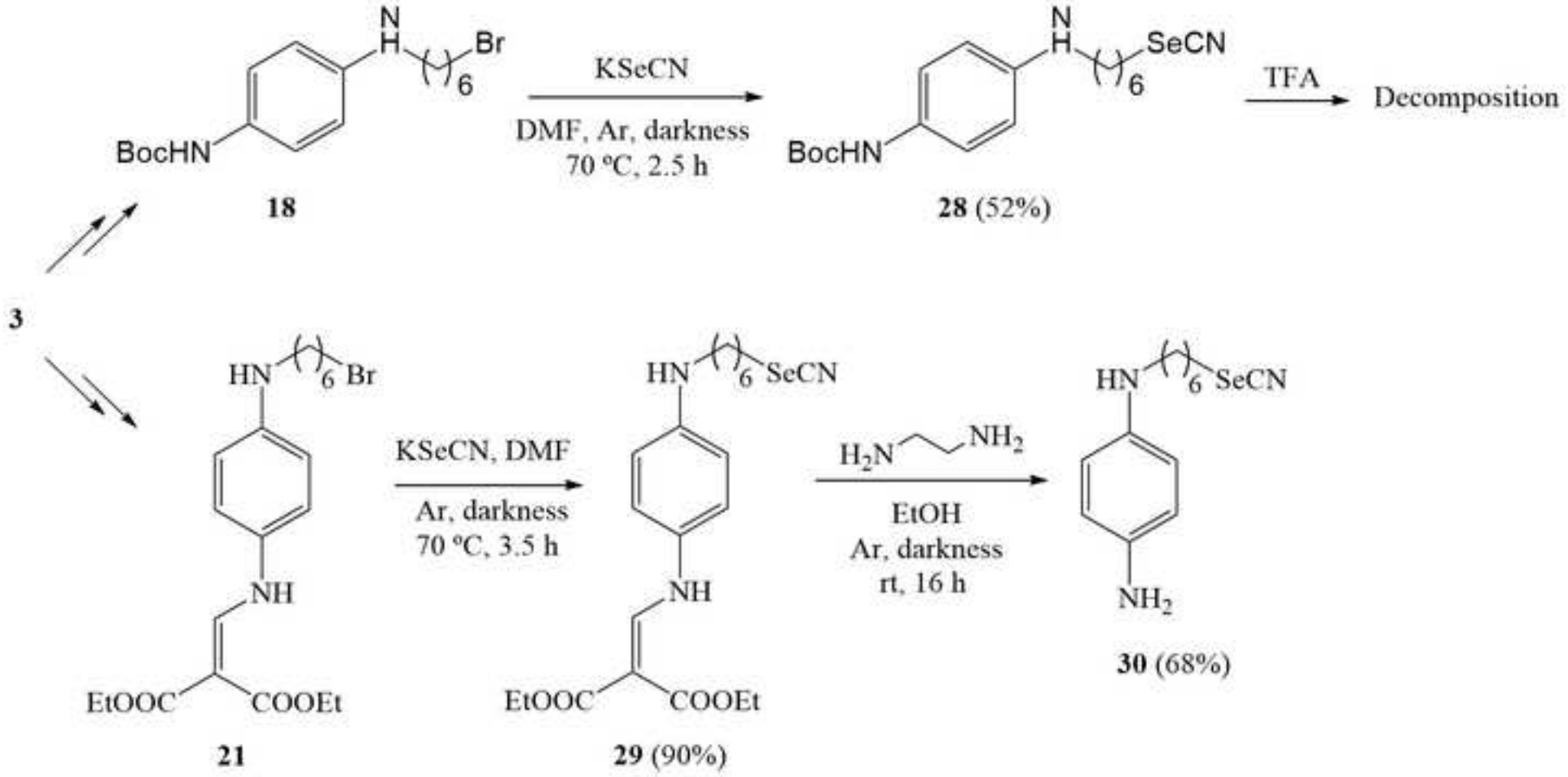

Scheme 8

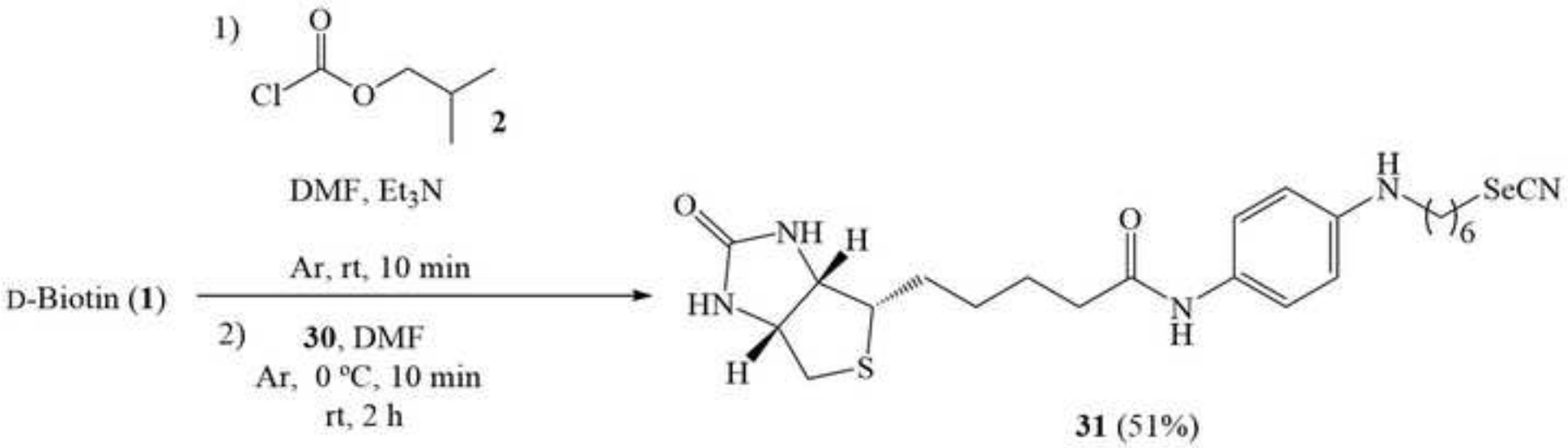

Table 1. Selected antiproliferative activities (GI_{50}, µM) against tumour and non-tumour cell lines[a,b]

Compound		**A549** (Lung)	**HBL-100** (Breast)	**HeLa** (Cervix)	**SW1573** (Lung)	**T-47D** (Breast)	**WiDr** (Colon)	**BJ-hTert** (Fibroblasts)	**S.I.**
Thiocyanate-NHBoc	**19**	14±2	16±3	19±4	16±3	18±6	29±7	n.t.	---
Thiocyanate-enamine	**22**	**2.7±0.6**	**3.5±1.6**	**3.4±0.6**	**1.8±0.6**	**4.9±1.4**	**5.0±0.6**	>100	>56 – >20
Thiocyanate-NH_2	**23**	**2.8±1.0**	**4.0±0.9**	**4.7±0.7**	**2.2±0.6**	17±4	15±3	>100	>36 – >6
Thiocyanate-biotin	**24**	29±11	19±1	6.3±1.7	22±2	34±4	36±7	n.t.	---
Disulfide-biotin	**25**	>100							
Selenourea-biotin	**27**	22±3	23±10	20±3	24±7	28±9	39±4		
Selenocyanate-NHBoc	**28**	**3.9±0.5**	**4.7±1.1**	**2.4±0.4**	**2.5±0.9**	**3.6±1.2**	**5.4±0.7**	>100	>42 – >19
Selenocyanate-enamine	**29**	**3.5±0.6**	12±2	13±3	**2.5±1.2**	16±4	18±6		>40 – > 2
Selenocyanate-NH_2	**30**	**0.21±0.00**	**0.18±0.01**	**0.086±0.019**	**0.13±0.03**	**0.026±0.011**	**0.12±0.06**	91±11	3500 – 433
Selenocyanate-biotin	**31**	**0.066±0.026**	**0.051±0.018**	**0.013±0.005**	**0.017±0.009**	**0.059±0.020**	**0.023±0.011**	>100	>7700 - >1515
5-FU		2.2±0.3	4.4±0.7	16±5	3.3±1.2	43±16	49±7	5.5±0.5	0.1–1.3
CDDP		4.9±0.2	1.9±0.2	1.8±0.5	2.7±0.4	17±3	26±4	14±2	0.5–7.4

Table 2. GI_{50} values (μM) for the antiproliferative activity of **31** in NCI-H460, NCI-H460/R, and MRC-5 cells					
Compound	**NCI-H460** (Lung)	**NCI-H460/R** (Lung)	**MRC-5** (Fibroblasts) (non-tumour)	**S.I.**	**Resistance factor** (NCI-H460/R / NCI-H460)
31	11.1±1.29	116.6±1.46	136.1±1.26	12	10.5

Biotinylated selenocyanates: potent and selective cytostatic agents

Jesús M. Roldán-Peña,[a] Adrián Puerta[b], Jelena Dinić,[c] Sofija Jovanović Stojanov,[c] Aday González-Bakker,[b] Francisco J. Hicke,[a] Atreyee Mishra,[d] Akkharadet Piyasaengthong,[d,e] Inés Maya,[a] James W. Walton,[d] Milica Pešić,[c,*] José M. Padrón,[b,*] José G. Fernández-Bolaños,[a,*] Óscar López[a,*]

The authors declare that they have no known competing financial interests or personal relationships that could have appeared to influence the work reported in this paper.

Click here to access/download

Video

Video S1.avi

Click here to access/download

Video

Video S2.avi